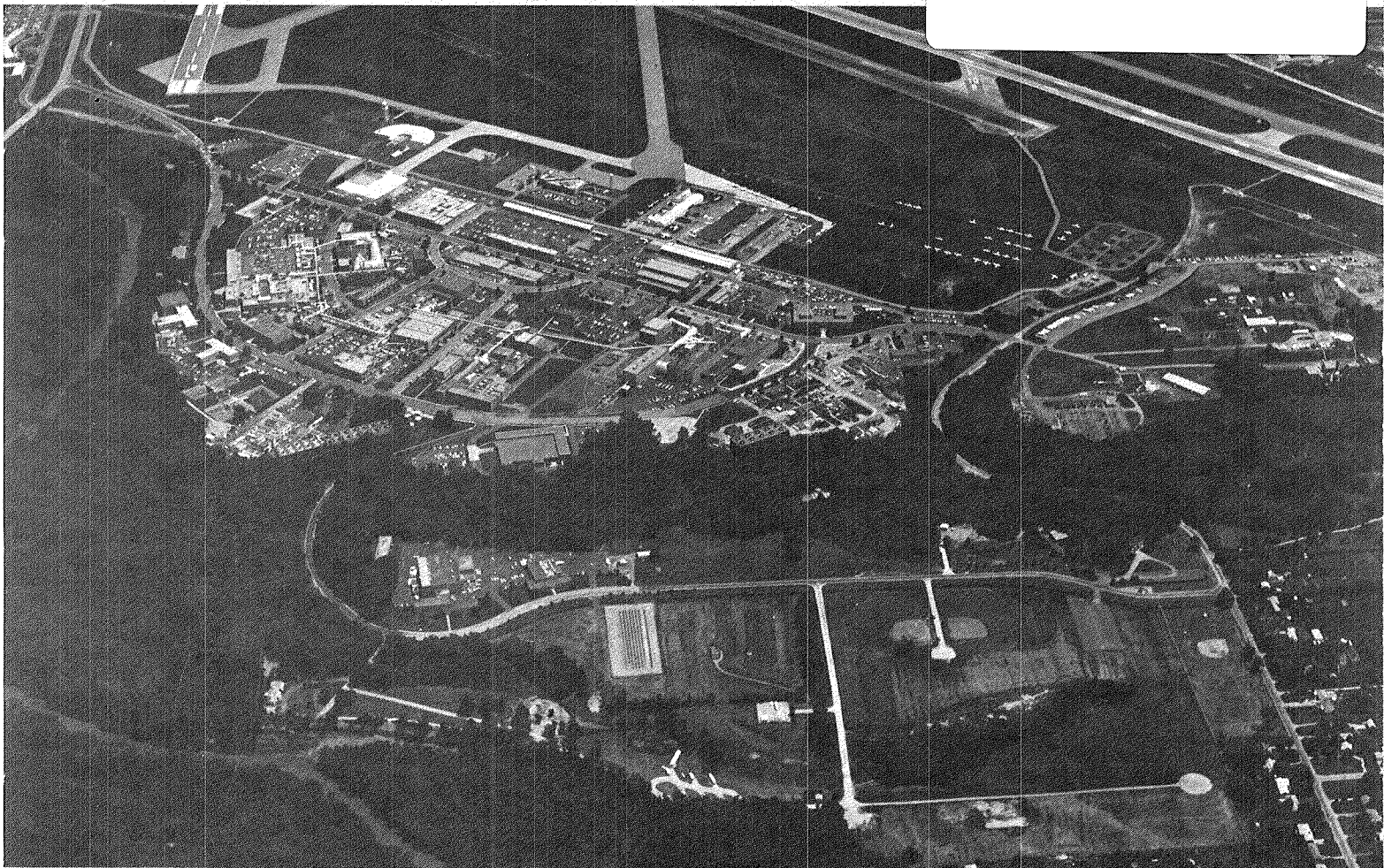


# Research and Technology Lewis Research Center

## Annual Report 1982

NASA-TM-83038 19830006898



**NASA**  
National Aeronautics and  
Space Administration

**LIBRARY COPY**

APR 18 1983

LANGLEY RESEARCH CENTER  
LIBRARY, NASA  
HAMPTON, VIRGINIA



NF00354

# Contents

---

Introduction..... 1

Aeronautics ..... 2

Space ..... 26

Terrestrial Energy ..... 38

# Introduction

---

This report presents highlights of the research accomplishments of the Lewis Research Center for fiscal year 1982. It is the sixth annual report in this series. The report is divided into three sections, covering aeronautics, space, and terrestrial energy. Each section of the report contains descriptions of progress in specific project activities as well as in basic research and technology activities. For example, materials work on aircraft turbine blades is reported in the aeronautics section. The Lewis Research Center is engaged in research—in support of NASA goals and objectives—in energy-conversion processes and systems for propulsion in the atmosphere, in space, and on the ground and for the generation and storage of electric energy for both terrestrial and space applications and in materials and structures for such systems.

Products of Lewis' research projects, used in both commercial and military aircraft and in space vehicles, have helped maintain the United States' preeminence in these fields. Work is also in progress to improve the efficiency of current energy-conversion processes and to develop hardware and systems to make use of alternative energy sources for flight and terrestrial applications.

This report describes 75 Lewis research projects that produced significant results in fiscal year 1982. The results of all research and technology work performed during the fiscal year are contained in 685 Lewis-published technical reports and presentations prepared either by Lewis scientists and engineers or by contractors.

An additional highlight of 1982 is that three Lewis products were selected for the Industrial Magazine IR-100 awards. Two of the awards, for a microwave ice accretion instrument developed by Ideal Research, Inc., and for an ultralightweight printed circuit developed by the Raytheon Co., both under contract to Lewis, are highlighted in this report. The third award, for the so-called CLEFT process of fabricating solar cells (cleavage of lateral epitaxial films for transfer), was described in the 1981 R&T Report and is not repeated this year. In summary, however, this process yields gallium arsenide solar cells that are 80 percent thinner and 75 percent lighter than the thinnest silicon solar cells currently available. The Lewis contact for information about the CLEFT process is Irving Weinberg, who may be reached at (216) 433-4000, Ext. 5295, or at FTS 294-5295.

For general information about the report, contact Robert Finkelstein at (216) 433-4000, Ext. 706, or at FTS 294-6706.

# Aeronautics

---

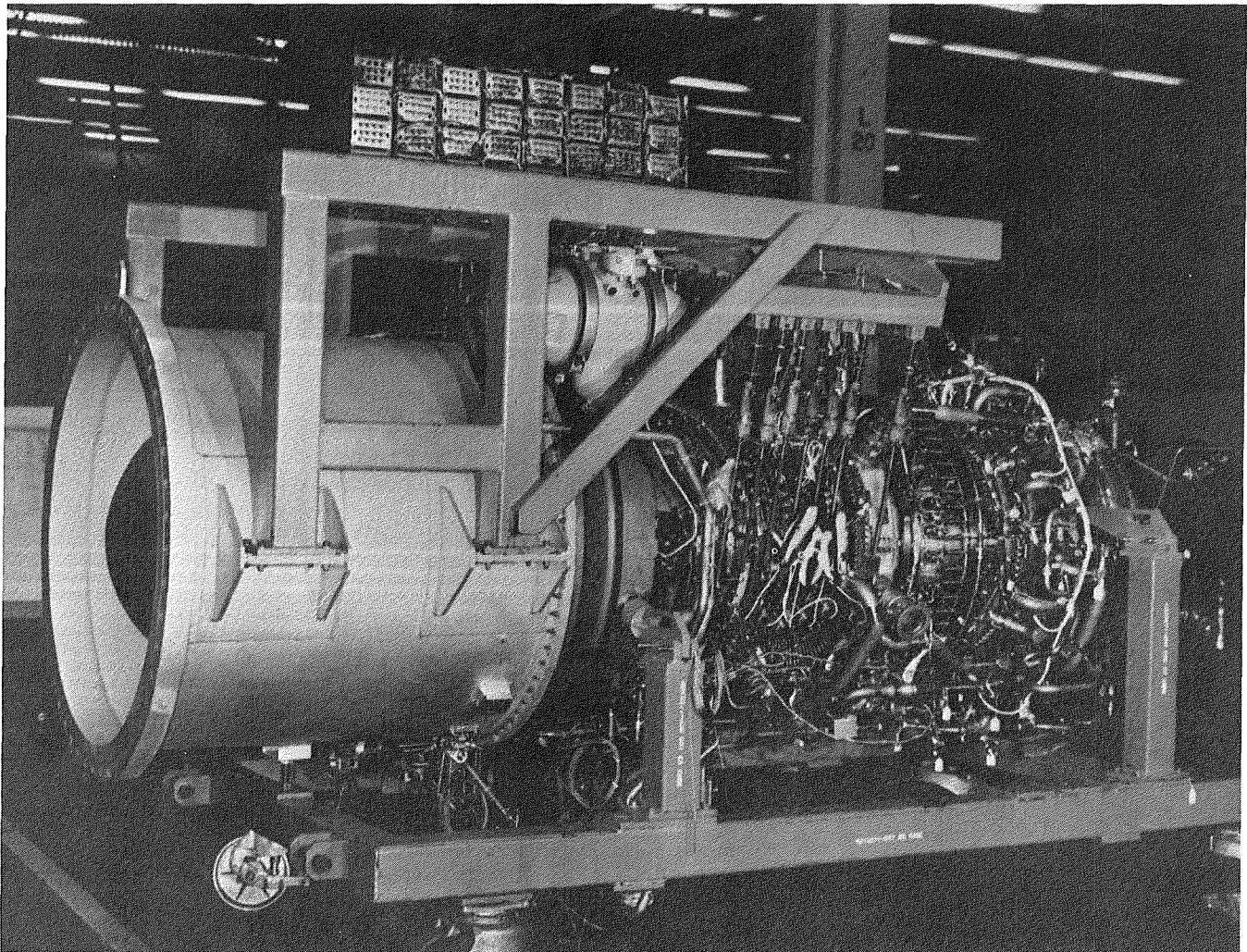
## IR-100

### Microwave Ice Accretion Meter (MIAM)

The formation of ice on aircraft surfaces is recognized as a serious problem, and various systems have been developed over the years to measure ice thickness. Recently, Ideal Research, Inc., under contract to Lewis developed a microwave ice accretion meter (MIAM) that measures the thickness of ice forming on a surface. Other such instruments use probes that project from the surface, thus making it necessary to infer how much ice is on the surface.

The MIAM detects the onset of icing, continuously monitors ice thickness, and displays ice thickness and accretion rate. A small (1.4 in. by 0.4 in. by 0.2 in.) microwave surface waveguide is mounted flush with the surface to be monitored. Ice forming on the surface of the waveguide causes its resonant frequency to shift. This shift in frequency is measured by a microprocessor and converted to a dc voltage proportional to the ice thickness. The microprocessor also computes the change in ice thickness with respect to time to get the ice accretion rate.

This instrument can monitor ice buildup on aircraft components before takeoff as well as in



*Energy Efficient Engine core test vehicle*

---

flight. It also could be mounted on a helicopter rotor blade. MIAM has received an IR-100 award.

### **Energy Efficient Engine**

Savings of at least 15 percent in fuel usage and approximately 10 percent in direct operating costs are projected for future transport aircraft using advanced-technology engine components developed under the Energy Efficient Engine Program.

Under contracts from Lewis, both the General Electric Co. and Pratt & Whitney Aircraft (UTC) continued to develop and integrate advanced-technology engine components in 1982. Component research was successfully completed. Through additional experimental evaluations of two high-pressure-ratio, 10-stage compressor designs, advances in compressor efficiency and pressure ratio were validated. Testing of a full-scale, single-stage, high-pressure turbine substantiated advanced transonic aerodynamic performance predictions. The high-pressure-ratio core engine tests were also successfully completed. The high component efficiencies achieved in previous components tests were maintained in the core engine environment. Excellent operating characteristics and efficiencies were achieved over a wide range of power settings, including startup, and this demonstrated the complete compatibility of the advanced-technology compressor, combustor, and turbine.

### **Combustion Systems for Broadened-Property Fuels**

Current jet engine combustion systems use relatively high-quality fuels, essentially kerosenes obtained by straight distillation of crude oil. The availability of such high-quality fuels obtained with minimum refining is expected to diminish toward the end of this century because of diminishing supplies of suitable crude oils. In fact, a reduction in fuel quality has been gradually taking place for several years because of changes in the sources of crude oil.

As the availability of high-quality jet fuel obtained with present refining techniques decreases, the options seem to be either to resort to more extensive refining at higher cost and energy consumption or to modify jet engines, particularly combustion systems, to use fuels with less stringent specifications. Such fuels are referred to as "broadened-property fuels."

Unfortunately a number of problems, such as a significant increase in combustor metal temperature, increased emissions of pollutants, and fuel system plugging with carbon deposits, need to be solved in order to use these fuels successfully.

Under parallel contracts to Lewis, the General Electric Co. and Pratt & Whitney Aircraft (UTC) have developed combustion systems for broadened-property fuels. These systems have demonstrated the potential to significantly reduce the effects of the use of broadened-property fuels. One of the most promising concepts uses variable geometry to optimize combustion conditions over the entire operating range of the jet engine. This results in lower sensitivities of metal temperatures and pollutant emissions to changes in fuel properties. Other advanced combustion system concepts that use multizone burning have also been evaluated, along with numerous modifications involving fuel-injection and metal-cooling techniques. The better designs that have been identified as having the potential for successfully using broadened-property fuels are being further refined by both companies in the second phase of this program.

### **Three-Dimensional Compressible Flow Analysis for Propellers**

Classical propeller analyses are based on incompressible flow assumptions with corrections for compressibility. A new method of analysis, begun by Ames and completed by Lewis, was developed that rigorously includes compressibility effects and predicts both the location of shock waves and strength during high-speed operation. A new computer program (NASPROP-E) was written that solves the three-dimensional compressible (inviscid) Euler equations for the steady flow around high-speed propellers. The propeller blades are represented numerically by parametric bicubic splines. The computational grid is formed by a simple geometric method that results in an "H" grid on the blade-to-blade surfaces. The unsteady Euler equations are written in a cylindrical coordinate system that rotates with the propeller blades and are then transformed to the computational plane. The resulting equations are solved in finite-difference form by using an implicit approximate factorization method.

This program is being applied to propeller configurations currently being studied for use at flight Mach numbers to 0.8. Analysis results are



indicating locations of shock waves, cascade effects, propeller-nacelle interaction effects, tip vortex formation, and three-dimensional flow features.

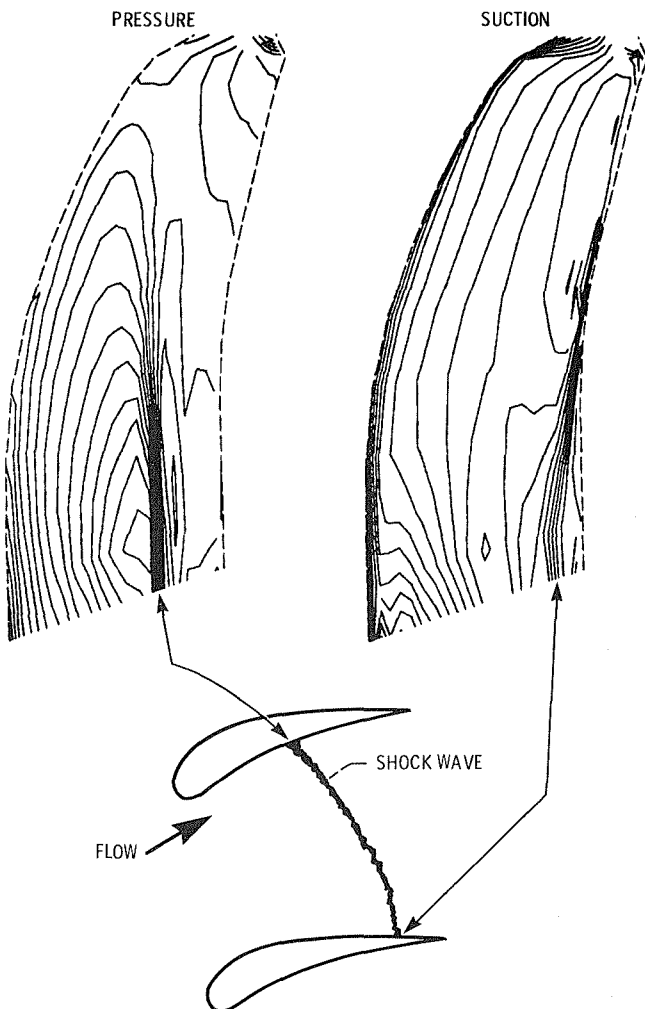
### New Flow Visualization Technique

Advanced propellers have the potential for achieving large fuel savings on future aircraft with high subsonic cruise speeds. The design of these new propellers is a challenging job that requires advanced computer analysis methods and new experimental test techniques. After the propeller is designed, models are tested in the wind tunnel to evaluate their performance potential. In these tests, flow visualization techniques are important

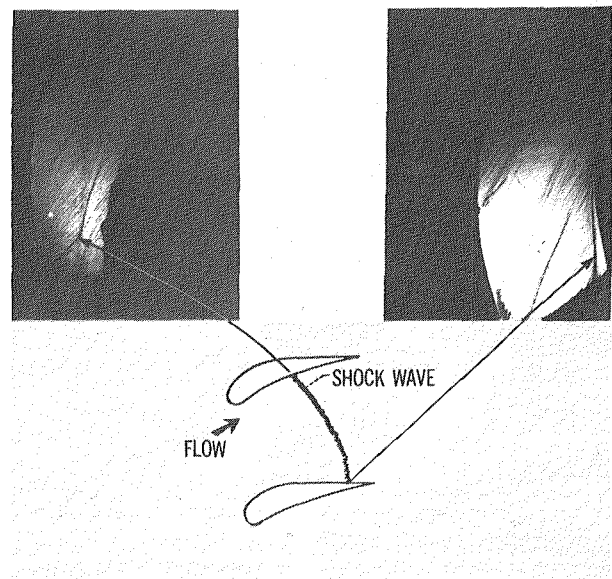
to help interpret the complex flow field between the rotating propeller blades. A new "paint flow" visualization technique developed by Lewis shows the flow field on the surface of the propeller blades. This new technique can be used to locate separated flow regions and shock wave structures on rotating blades. It is therefore a new diagnostic tool to help solve propeller design problems.

The "paint flow" technique consists of painting the propeller with a red undercoat and a white overcoat. When the propeller is at the desired operating conditions, solvent is injected into the wind tunnel. The solvent impinges on the rotating propeller blades and causes the paint to flow, leaving an airflow pattern on the surface of the blades.

This technique was first used to determine the exact reason for a rapid decrease in the performance of a 10-blade propeller above a Mach number of 0.75. The resulting pattern illustrates strong shock waves on the inboard portion of the blade and thus indicates a hub choking problem. The results of the "paint flow" technique and new computer analyses are being used to design propellers that will minimize this compressibility loss problem.



Lines of constant Mach number



Paint-flow-technique showing interblade shock wave structure

---

### **Cascade and Sweep Effects on Advanced Turboprop Flutter**

The advanced turboprop blades being developed at Lewis require swept, twisted, thin airfoils to attain high efficiency and low noise characteristics. This complex geometry can result in aeroelastic phenomena not found in current propellers. As part of the total advanced turboprop research effort, an analytical investigation emphasizing the effects of sweep and cascade aerodynamics on flutter was conducted.

The effects of sweep were studied by extending the techniques developed for fixed wings to rotating propellers. It was found that increasing the sweep could have a significantly destabilizing effect. Cascade effects were studied by coupling turboprop unsteady cascade models with propeller structural models. Even though the advanced turboprop blades were spaced relatively far apart, the cascade effects were found to be strong and destabilizing.

When both of these effects were included in the flutter prediction system, good agreement was found between the measured and predicted flutter boundaries. As a result, the contractor has included these effects in his design analysis system, and future designs will have a lower probability of encountering unexpected flutter problems.

### **Flow-Field Measurements in a Transonic Fan Stage**

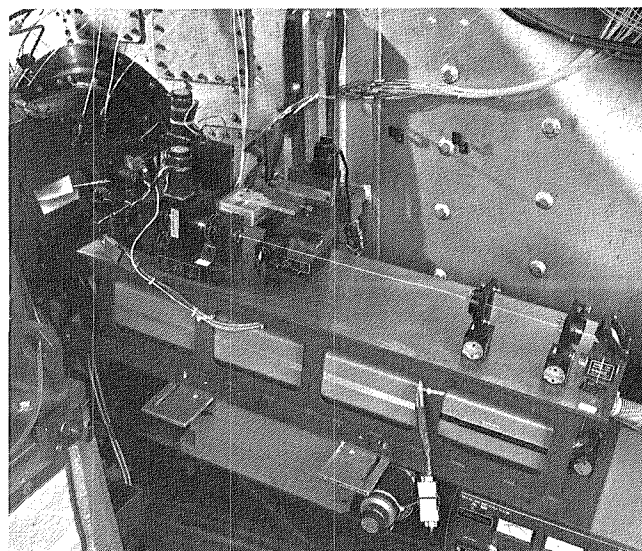
Measurements of the flow field within a transonic, axial-flow fan stage have been obtained by using an advanced laser Doppler velocimeter (LDV) system. The flow field ahead of, within, and downstream of the fan rotor has been surveyed over the full blade span with the fan stator removed. The resulting data represent the most complete survey of a transonic rotor blade flow field obtained to date and will be used to verify two- and three-dimensional flow analysis codes.

With the fan stator present, measurements will be made in the interblade space between the rotor and the stator as well as within and downstream of the stator. These measurements will represent the first U.S. effort to survey the unsteady stator flow field by using LDV techniques. The resulting data will be used to determine the effects of the unsteady rotor exit flow on the aerodynamic performance of the stator and the effects of the stator on the rotor

performance. The data will also be compared with high-response pressure measurements made during radial traverses of the flow field between the rotor and the stator. These comparisons will attempt to resolve differences noted in the past between results obtained from advanced measurement techniques and from conventional pitot-static pressure measurements.

### **Bird Impact Analysis Package for Turbine Engine Fan Blades**

A significant factor in the design of an aircraft gas turbine engine is adequate foreign object damage (FOD) tolerance. The component in a modern engine that is first struck by an ingested object, and that absorbs most of the impact, is the fan stage. Of those objects that are ingested reasonably often (including small rocks, hailstones, and scattered debris) the most damaging is probably a medium to large bird. Though the damage from harder objects can be severe, the objects themselves tend to be smaller than a fan blade, and thus the damaged area also is usually small. Often this damage is discovered only during ground inspection of the engine. On the other hand, birds can be relatively large, up to a few pounds, with a comparatively large impact area. Along with severe local damage near the leading edge of the blade, bird strikes can also produce loading near the root of the blade great enough to cause the blade (or blades) to break free.



*Laser Doppler velocimeter system in operation*

An analysis package has been developed to provide an effective and efficient means for analyzing the overall response of fan blades to bird strikes. The package is composed of two key elements: (1) A modal analysis of the fan blade and (2) an interactive bird strike analysis computer code. The modal analysis for this package is generated by NASTRAN. The bird strike analysis is based on a modified form of a computer code (Interactive Multi-Mode Blade Impact Analysis, MMBI) developed under contract for NASA. This code uses a fluid jet model for the bird and models the dynamics of the fan blade from a supplied geometric description and modal analysis. As the bird strikes the blade, the pressure loading during a given time step is calculated and decomposed into modal components. This loading is then used to numerically integrate the modal equations of motion over a time step. One of the key features of the analysis package is that the NASTRAN finite-element model and modal analysis are automatically integrated into the bird strike analysis code.

### Finite-Element Simulation of Turbofan Noise

To predict the sound field radiated from a turbofan inlet, a finite-element integral technique has been developed in conjunction with the Georgia Institute of Technology. The velocity potential formulation for the mean flow equations as well as the acoustic wave equation was employed in the program. The program first calculates the mean flow distribution for the inlet. Next, the mean flow solution is used in the

acoustic wave equation. To solve the acoustic wave equation, the sound field is divided into two regions: the sound field within and near the inlet, which is computed by using the finite-element method, and the radiation field beyond the inlet, which is calculated by using an integral solution technique. Numerical interaction between the interior and exterior regions is required to obtain a continuous acoustic field across the interface.

As seen in the accompanying figure, the interior portion of the test JT15D inlet has been divided into a number of triangular Hermitian elements. For clarity, the number of elements shown has been greatly reduced from the actual number used. The Hermitian formulation forces continuity of both the velocity potential and its derivatives at the nodes, thereby reducing the number of elements required to accurately predict the sound field. In the integral technique, Green's theorem is used to transform the wave equation in the external region into an equivalent problem of solving an integral equation over the boundary of the region designated by asterisks (\*) as shown in the figure. The iteration procedure between the two regions requires the acoustic impedances at the interface to be identical.

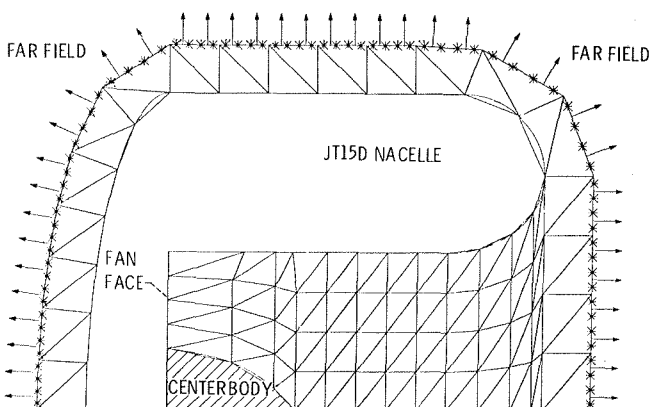
For some single-mode JT15D turbofan engine data, theory and experiment were found to be in good agreement for the far-field radiation pattern as well as for suppressor attenuation. The computer program can also be used to simulate flight effects that cannot be performed on a ground static test stand.

### Catalytic Combustors for Gas Turbine Engines

The control of emission levels of gaseous pollutants from aircraft and industrial gas turbine engines has been studied extensively by Lewis personnel. Methods of minimizing nitrous oxide ( $\text{NO}_x$ ) emissions have received significant attention.

One method that produced very low levels of  $\text{NO}_x$  in laboratory tests is catalytic combustion. Catalytic combustion makes it possible to use low fuel-air ratios, which result in relatively low combustion temperatures and consequently impede the formation of  $\text{NO}_x$ .

Under a multiphase program funded jointly by Lewis and the U.S. Air Force, the General Electric Co. generated advanced catalytic combustor concepts. Guidelines for combustor size and engine cycle were based on values from the Lewis Energy Efficient Engine Program. Concepts were analytically assessed to ascertain their



*Division of JT15D inlet into Hermitian triangular elements*

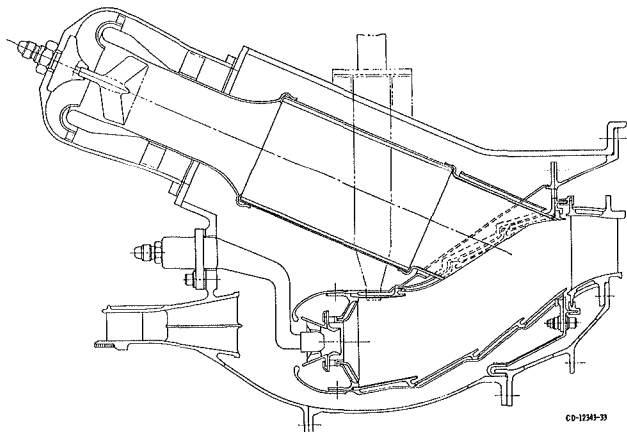


potential for satisfying practical operating requirements.

The two most promising concepts developed by General Electric were experimentally evaluated in sector configurations to assess their potential for use as future advanced aircraft combustors. Each concept used a catalytic reactor as a main stage along with a conventional pilot. Evaluation was limited by the maximum temperature limit of state-of-the-art reactor substrate materials. However, excellent operation was achieved at 60 percent power, cruise, climb, and takeoff inlet temperatures (860° to 1005° F) for the reverse-flow catalytic combustor concept. Reactor temperatures were 2540° F and reactor total-pressure drop was less than 5.5 percent. High combustion efficiency, ultra-low NO<sub>x</sub> pollutant levels, and very low smoke values were achieved with Jet A fuel.

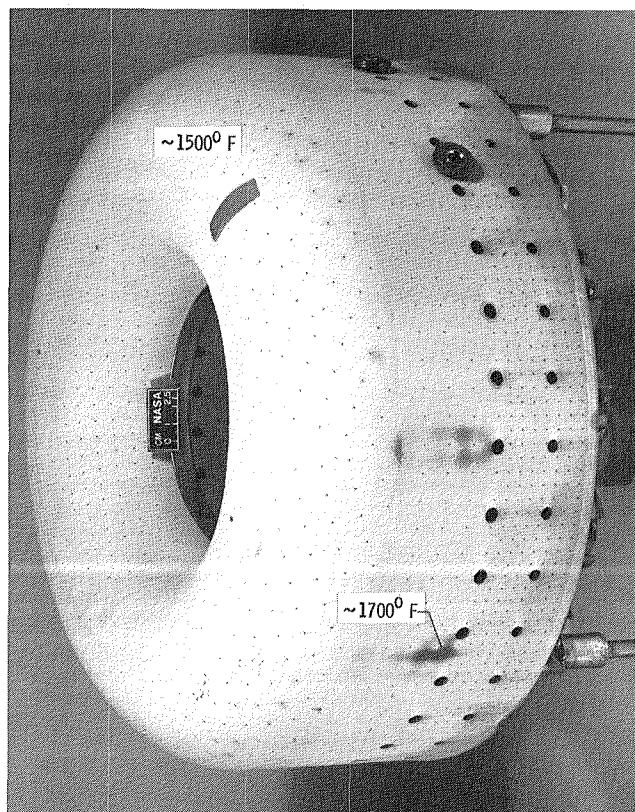
### Combustor Liner Cooling Technology

Combustors for high-performance, gas turbine aeronautical engines currently operate at the limits of present-day materials. As a result, the durability of combustor liners is a significant problem. These liners are typically cooled by films of air passing over their surfaces. The problem of liner durability is especially acute for small combustors of the type used in general-aviation aircraft, rotorcraft, and commutercraft, as these combustors have higher ratios of surface air to volume than do larger designs. Durability problems are expected to worsen because future mission trends project higher pressure ratios, more intense combustor burning, and less air available for liner cooling.



*Can-annular, reverse-flow, parallel-stage catalytic combustor*

Advanced liner research is in progress at Lewis. This research is aimed at replacing the conventional film-cooling approach with approaches that use available coolant air more efficiently or incorporate advanced materials. One advanced approach that is yielding very promising results is transpiration cooling of combustor liners. This approach uses the heat-sink capacity of the coolant and more uniformly distributes coolant over liner surfaces. Experimental evaluation of a full-size combustor constructed of the transpiration material Lamilloy, a Detroit Diesel Allison trademark, demonstrated the following results: (1) The transpiration-cooled liner used 50 percent less coolant than a film-cooled liner, with no increase in liner temperature; (2) redirecting the "saved" coolant air to other purposes gave considerably better uniformity in combustor exit temperature pattern and reduced NO<sub>x</sub> pollutants by 35 percent; and (3) existing combustor design correlations can be used to incorporate transpiration cooling.



*Lamilloy combustor liner wall temperature indication at sea-level takeoff. Design temperature, 1700° F.*

### Primary Zone of Small Gas Turbine Combustor

For many aeronautical engine applications, designers of small gas turbine engines prefer a close-coupled, compressor-to-turbine shafting arrangement. In most cases, this necessitates the use of a reverse-flow annular combustor. A design methodology for obtaining the maximum performance potential of these combustors is needed because the design tools currently available are inadequate. As a result, much time and cost is expended through "cut and try" approaches to achieving the desired performance.

The development of combustor design tools through analytical design methods and experimental verification is being studied at Lewis. In one such activity sponsored by Lewis and the U.S. Army, Detroit Diesel Allison recently upgraded an existing three-dimensional reacting combustor flow model incorporating variable finite differences. The procedure was to upgrade the model by incorporating geometric subroutines, reducing computing time, and evolving graphic subroutines to clearly display results. The model was then employed to define conceptual modifications that would improve the performance of an existing combustor. The concept was evaluated in a component test rig, and experimental results were compared with analytical predictions. Unique experimental instrumentation included probes at the end of the primary zone to record fuel-air distribution.

Although limited by the current state of the art in analytical modeling, this study demonstrated the high potential of this approach to combustor design tools. Required combustor performance levels were achieved, and analytical predictions agreed well with experimental data.

### Turbine Bypass Concept

Propulsion systems for future aircraft will be required to operate efficiently at extreme throttle settings. For example, the engines will be at high throttle during the supersonic climb and cruise of a fighter but will be throttled back considerably for subsonic cruise. With conventional engines, low-throttle operation is generally inefficient and incurs a considerable increase in inlet spillage and drag. The turbine bypass concept allows the engine to operate efficiently at low throttle and eliminates engine-related drag.

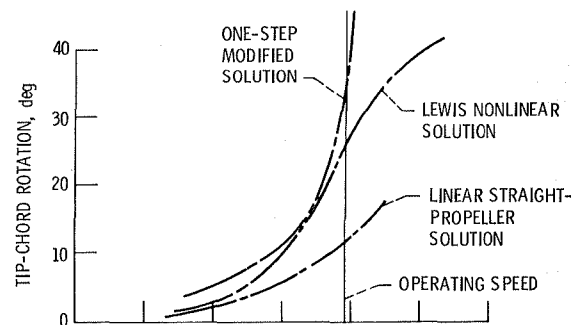
This concept features an undersized turbine designed for low-throttle operation. At low throttle, all of the compressor discharge air goes

through the combustor and the turbine. At high throttle, some of the compressor discharge air is bypassed around the combustor and the turbine and injected into the nozzle. This arrangement allows the compressor to operate at a single operating point for all throttle settings. Thus, the engine rotational speed remains high for low-power settings and operates at the most efficient point for all throttle conditions. High airflow is maintained, and this eliminates throttle-dependent losses.

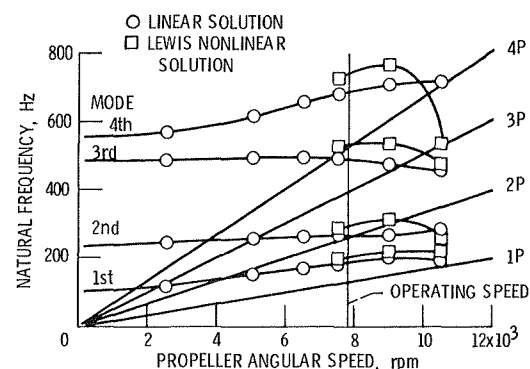
Contracted and in-house studies indicate that the turbine bypass turbojet is attractive in terms of mission performance, fuel efficiency, and simplicity. The turbine bypass concept may have application for other aircraft propulsion systems where wide variations in throttle setting are required, such as for helicopters and VTOL aircraft.

### Nonlinear Structural Analysis of Propellers

Advanced propeller concepts for transport aircraft feature thin, highly swept and twisted propeller blades to achieve high efficiency and



Tip-chord rotation predicted by various methods



Nonlinear structural response of swept, twisted propellers

low noise at cruise. Deflections due to centrifugal loading, for blades of this type, exhibit a high degree of nonlinearity and thus require special analysis techniques not automatically available. Analysis indicates that these blades may experience an abrupt reversal of tip deflection or a large change in tip-chord angle as the rotational speed is increased. Evaluation of these position changes early in the design phase is important because of the possible severe effect on aerodynamic performance. Therefore, a "user friendly" procedure was developed at Lewis for the nonlinear analysis of swept, twisted propellers. Unlike other approaches that make a one-step modification to the analysis, the Lewis procedure corrects the blade geometry at each load step to more accurately represent the nonlinear effects. Comparison of results with other solutions shows that the prediction of tip-chord angle and natural frequencies can be erroneous if geometry-updating procedures are not used.

#### **Reproducible Growth of Single-Crystal Silicon Carbide**

There is a critical need in a number of fields for semiconductor electronics capable of operating at high temperatures (500° to 1000° C). Two of these needs are for signal-conditioning electronics in aircraft engine turbines and for high-reliability electronics in aircraft engine controls. Silicon carbide (SiC) has long been recognized to be the theoretically nearly optimum high-temperature material. However, more than 20 years of effort in this country and many others failed to yield a process for reproducibly

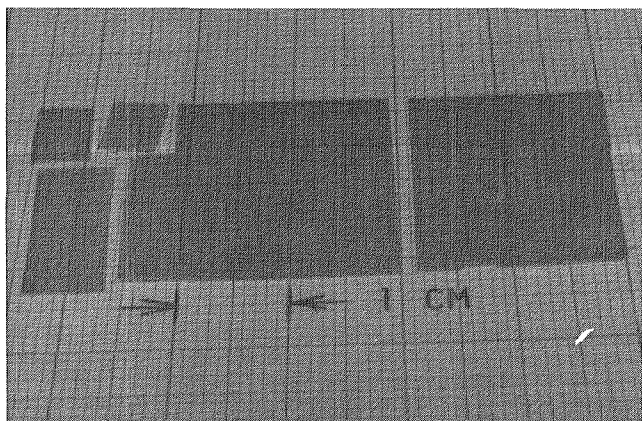
fabricating semiconductor-quality single crystals of SiC. We now have such a process.

A National Research Council research associate from the University of Kyoto was brought to Lewis because of a novel idea for a crystal growth process that he had published. He and Lewis physicists carefully modified and implemented this process until we can now reproducibly obtain high-quality single crystals of 5-cm<sup>2</sup> area by 30-cm thickness. Devices fabricated from these crystals should open the door to electronic applications at temperatures exceeding 500° C.

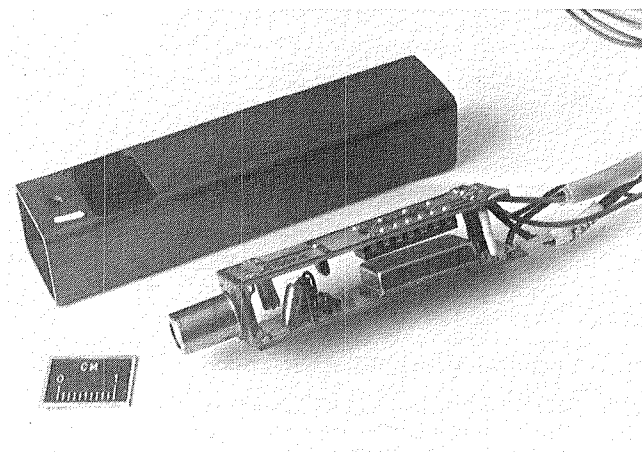
#### **Optical Probe for Turbine Engine Blade Vibrations**

Highly sensitive, low-power, solid-state probes with a light-emitting diode and a photodiode receptor can be used to measure turbine blade vibrations. The receiver and the emitter share a common lens as well as the necessary signal-processing electronics in a self-contained and shielded package. These probes are more reliable and easier to use than alternative approaches based on fiber-optic bundles and photomultiplier sensors. The small size and modular nature of the resulting probe package allow many of these probes to be readily mounted on casings in order to measure the vibrations of all blade tips on a spinning rotor simultaneously.

The emitting diode within the probe provides a focused beam of light that is reflected back to the photodiode when a blade tip passes. Signal-processing circuits provide a digital logic signal when the blade is detected. Blade tip deflections are calculated by a digital system that determines



*Cubic silicon carbide single crystals*



*Optical probe*

the time at which a blade passage occurs and subtracts the time when the blade passage would have occurred if there were no tip deflection. Repeatability of the probe's response has been demonstrated to be well within the minimum time resolution of the digital system (30 nsec). Blade tip deflections of 0.0005 in. are measurable with an 1800-rpm, 20-in.-diameter-blade rotor.

Three adjacent probes can be placed to measure three points on the chord of every blade. With data reduction, overall blade bending, torsion, and chordwise bending vibration patterns can be determined.

### Turbine Engine Rotor Computer Code

In a typical aircraft gas turbine there are many instances in which rotor-case rubs can occur. When a rotor rubs on the case, a frictional force is generated that can drive the rotor to whirl in the direction opposite to the direction of rotation, and this is known as backward whirl. It can occur at very high speed and with ever-increasing rub force; thus, rubs can be dangerous.

A method for direct integration of a rotor dynamics system experiencing a blade-loss-induced rotor rub was developed. The method included a vastly improved numerical integration algorithm and resulted in a numerically stable computer code with short running times. The stable integration allowed many revolutions of the rotor to be accurately simulated, along with very short-duration rub forces. A new class of potential rotor dynamic instability due to rubbing at blade seals was identified with this computer code, it explained previously anomalous rotor instabilities.

This is the first time backward-whirl instability has been simulated. This new analytical tool provides information that will allow the design of rotor surface rub systems that minimize the possibility of catastrophic rub-induced rotor system failures.

### Simulations of Temperature Disturbances on Turbine Engines

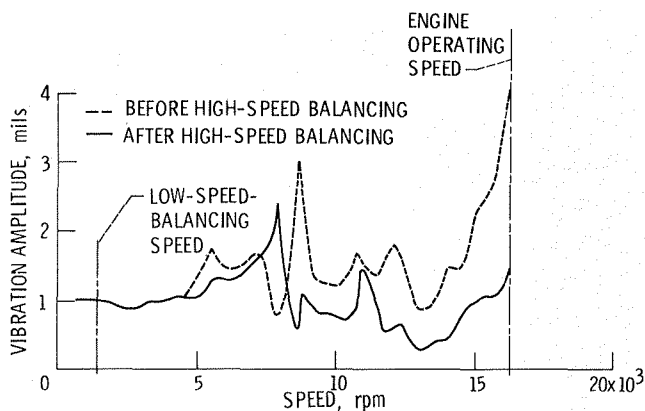
Incidents of nonrecoverable engine stall induced by gas ingestion have been identified and documented in flight tests of military aircraft. Experimental investigations to define details of the problem require duplication of the triggering mechanisms. Experimentally obtained information can then be used to guide, extend, and validate analytical models being established by both the U.S. Air Force and NASA.

The thermal effects of such ingestion can be simulated with a new gaseous hydrogen burner. Such a burner has been developed for use in the inlet plenum of a Lewis altitude test chamber. The burner demonstrated the ability to generate rapid temperature transients exceeding 4800° R per second. The ability to generate nonrecoverable compressor stall of an engine was also demonstrated.

### High-Speed Balancing of Turbine Engines

A facility for high-speed balancing of helicopter turbine engines has been developed and delivered to the U.S. Army overhaul center at Corpus Christi, Texas. The system spins engine shafts at their normal operating speed, 16,000 to 21,000 rpm, and thus allows correction of out-of-balance conditions that cannot be detected by customary low-speed balancing (1500 rpm). The accompanying figure compares vibration amplitude after high-speed balancing with that after low-speed balancing. The improvement is pronounced at the normal engine operating speed. In the balancing system the engine shaft is driven by a variable-speed electric motor driving through a speed-increasing gearbox. The shaft is spun in an evacuated enclosure to reduce windage losses so that a low-power drive system is adequate. A minicomputer automatically acquires shaft vibration data and calculates balance corrections.

Use of high-speed balancing is expected to increase the acceptance rate of newly overhauled engines, as well as to provide overall smoother engine operation. This technology is already being adopted by the U.S. Army and the Air Force. Cost savings will also result as low-speed



Results of high-speed balancing on turboshaft engine

balancing operations can be reduced or eliminated. An annual saving of \$500,000 is projected for the operation of one cell at the Corpus Christi Army Depot.

### Advanced Rotary Telemetry System

Transferring temperature, strain, and pressure data from the rotating parts of a turbine engine is a difficult task. The techniques most often used are slip rings and telemetry systems. The need for more channels of data from the rotating parts of smaller, higher temperature, and higher rotational speed engines has necessitated improvements in existing telemetry technology.

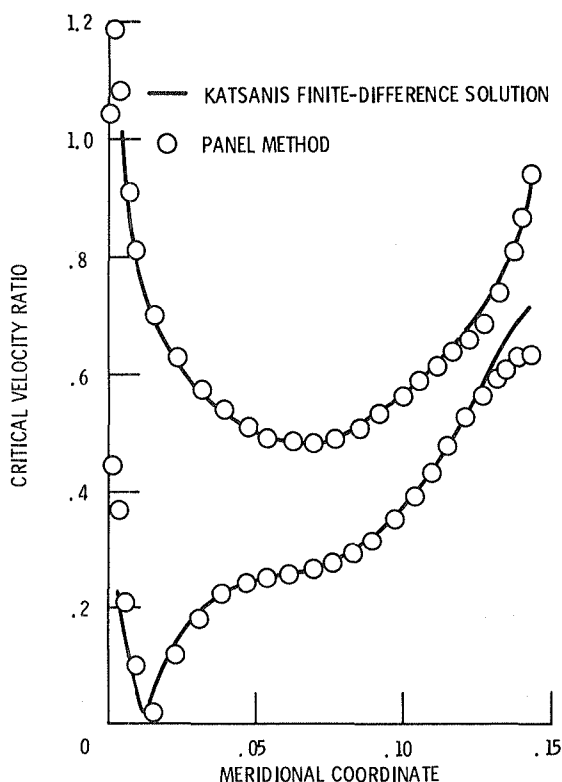
A program was started to develop an advanced telemetry system using new integrated-circuit and materials technologies now available. The development effort resulted in a lightweight (5 g) single-channel transmitter module. Its operation is based on a frequency synthesizer technique and is capable of 50-channel-per-system transmission at 150° C and 50,000 g's of rotational

acceleration. The module construction uses hybrid electronics on a polyimide substrate and a graphite-fiber lid. Performance tests were completed on an engineering model system that included multiple transmitters, antennas, and receivers, a power supply, and a titanium test rotor.

### Turbomachinery Panel Method

An improved panel method or integral equation solution has been developed for calculating cascade flows on a surface of revolution. The method adapts advanced integral equation solution techniques developed for external flows to the internal flow problem. Approximate governing flow equations are solved for fixed or rotating blade rows. The effects of compressibility, radius change, and variable stream sheet thickness are included in the solution. The major advantages of the panel method over previous finite-difference and finite-element methods are its rapid calculation time (typically less than 4 CPU sec on the IBM 3033 at Lewis) and its ability to calculate flows about complex blade geometries. The main drawback of the method is that it will not predict shocked flows.

The panel method is intended primarily for use in preliminary design. Its speed and versatility make it a good candidate for use in interactive design systems. The method can be used in such systems to generate blade shapes and screen designs for analysis by more accurate, but longer running, flow analysis computer codes.



Comparison of methods for calculating cascade flows in radial inflow turbine

### Line-of-Sight Laser Anemometer

Detailed flow measurements in aircraft turbomachinery components are needed to validate new three-dimensional computer codes. Laser anemometry is being used to provide flow velocity measurements. However, conventional fringe anemometers measure only velocity components normal to the optical axis. A laser anemometer was developed using a confocal Fabry-Perot interferometer to measure the line-of-sight velocity component (i.e., the component along the optical axis). This instrument directly measures the Doppler shift of laser light scattered from small particles injected into the flow. The measured Doppler shift is proportional to the velocity component along the optical axis. Both the mean line of sight and the turbulence intensity are obtained, even when the transverse velocity component is much larger than the line-



of-sight component. The anemometer was used to measure the radial velocity and turbulence intensity in a 0.5-m-diameter turbine stator.

### Holographic Motion Pictures

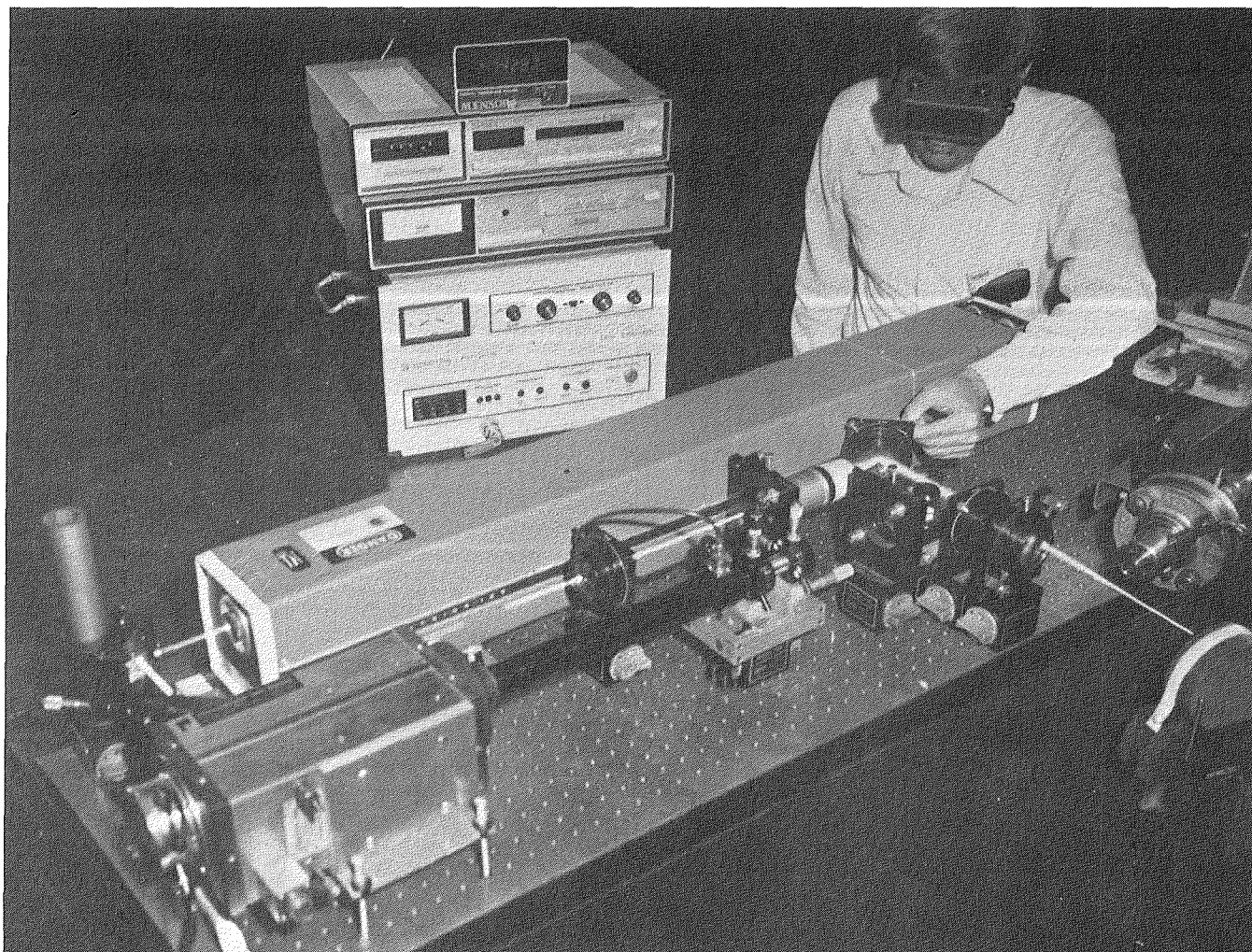
A technique has been developed to obtain 20 double-pulse holographic pictures per second. This process has been applied to obtaining three-dimensional motion pictures of the shock pattern motion that takes place between the blades of a flutter research facility. Previous techniques allowed less than 1 picture per minute. Now it is possible to correlate shock patterns and positions with blade position. This is accomplished by using a pulsed laser and an

aerial motion picture camera, both precisely synchronized with the blade motion.

### Flow Visualization of Turbulent Coaxial-Jet Mixing

Turbulent mixing of confined coaxial jets is being studied because of its similarity to combustor turbulent mixing. It is therefore of value in verifying mathematical models of combustor flow fields.

Under a contract from Lewis, the United Technologies Research Center performed experimental tests in which a fluorescent dye was uniformly dissolved in water and expelled through the center jet. The mixing of the dye stream with



*Line-of-sight laser anemometer*

the annular jet was carefully studied. The study used laser velocimetry (LV) and laser-induced fluorescence (LIF) to measure fluctuating velocities and concentrations. Mixing patterns were observed with high-speed motion pictures.

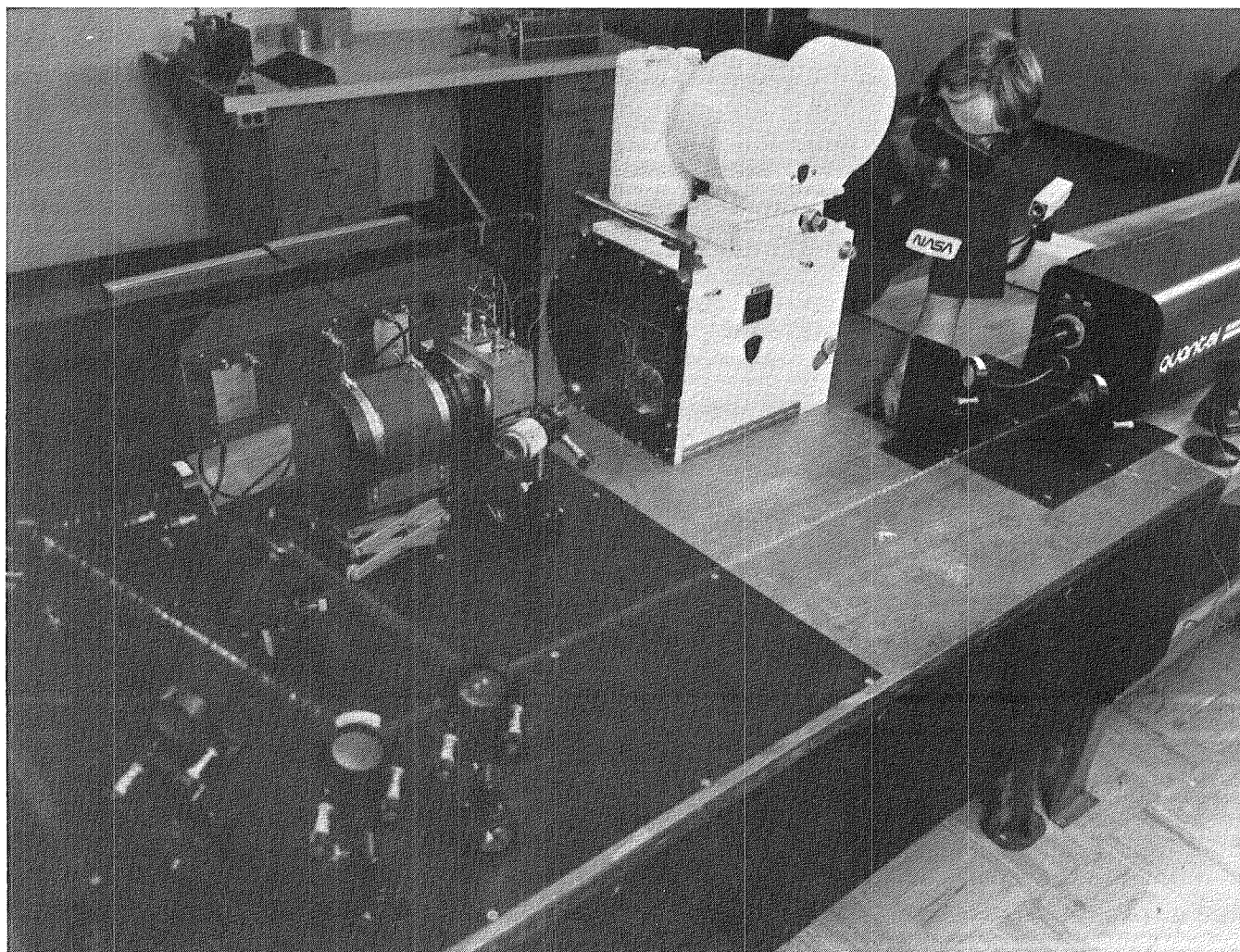
Flow visualization studies showed four major shear regions: a wake region immediately downstream of the inner-jet inlet duct, a shear region further downstream between the inner and annular jets, a recirculation zone, and a reattachment zone.

A combination of turbulent mass transport rate, momentum transport rate, concentration, and velocity data was obtained from simultaneous measurements with an LV and an LIF system.

Velocity and mass transport in all three spatial directions were measured. These data will be useful for model validation and improvement.

#### **Internal Flow in an Internal Combustion Engine**

A detailed study of flow patterns and turbulent kinetic energy distribution in piston-powered engines is required to provide an analytical basis for advanced concepts for achieving higher power with lower fuel consumption rates. As part of Lewis' internal combustion engine program for small aircraft and in collaboration with Carnegie-Mellon University, a computer code was developed that simulates two-dimensional flows



*Holographic motion picture system*



in a configuration consisting of an axisymmetric piston-cylinder with a moving valve. An implicit finite-difference procedure is applied and used to study the turbulent flow field in a motored four-stroke cycle engine. The procedure solves the conservation equations of mass, momentum, energy, turbulent kinetic energy, and dissipation rate of turbulent kinetic energy. The numerical method has been used to study the effects of speed, compression ratio, bore/stroke ratio, and intake flow angle on flow fields and the formation and destruction of vortices.

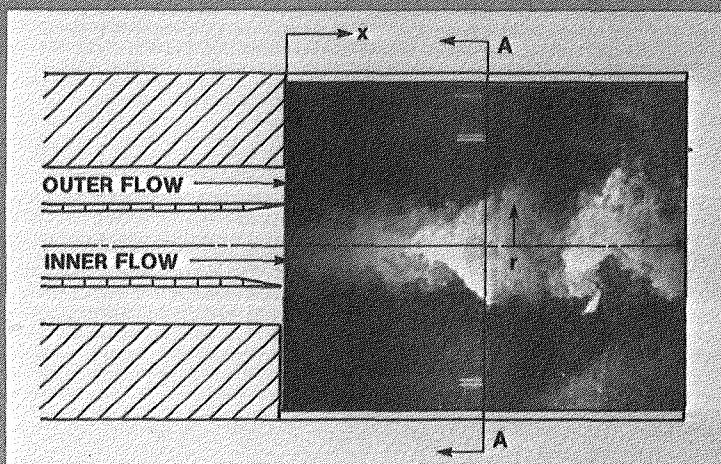
Comparison of the results of this numerical study with the experimental work of others showed good general agreement. Flow field plots and a computer-generated color motion picture were used to graphically display the results and to help analyze the location, dimensions, and interaction of the vortices.

### High-Temperature Photoswitch

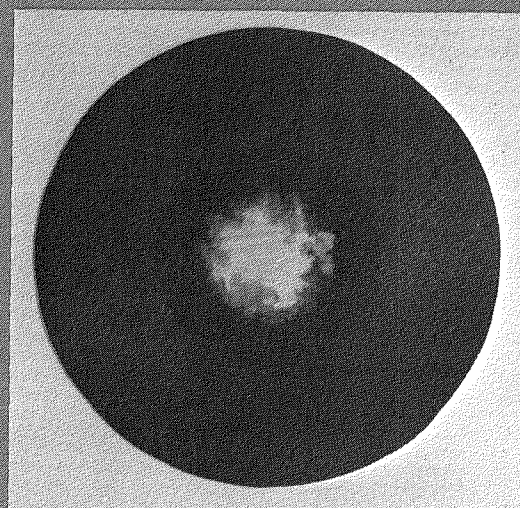
Electromagnetic disturbances such as lightning pose a threat to electronic control systems on aircraft engines. Protection can be provided by using shielded electrical cables, but the cables are heavy and bulky. Fiber-optic cables are a potential alternative to shielded electrical cables. Since optical fibers are immune to electromagnetic disturbances, the cables need not be shielded and can be made small and light.

To use fiber optics in engine control systems, one of the needed components is a photoswitch that can operate at temperatures as high as  $250^{\circ}\text{C}$ . The photoswitch would be used to control the electrical current supplied to actuators. The current could be switched on and off by using light transmitted over fiber-optic cables. Until recently, photoswitches that could operate at  $250^{\circ}\text{C}$  did not exist. However, the United Technologies Research Center, under

### WATER TUNNEL EXPERIMENT



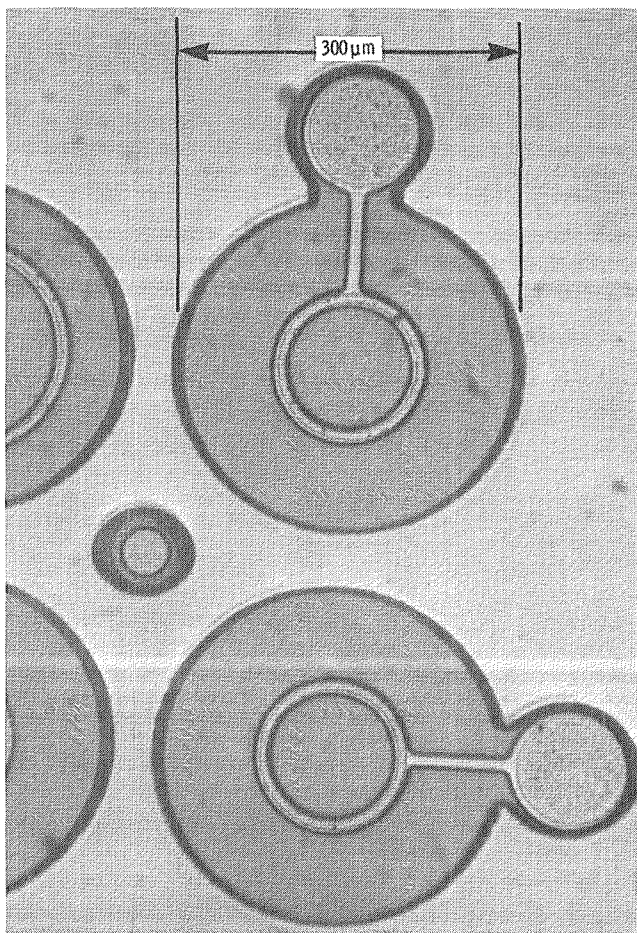
### SECTION A-A



contract to Lewis, has developed a gallium arsenide photoswitch with the necessary high-temperature capability. The central component of the photoswitch is a gallium arsenide phototransistor. During 1982, several phototransistors were fabricated and tested successfully at 250° C.

### High-Temperature Particulate Erosion Rig

Increased turbine thermodynamic efficiency and reduced maintenance costs are two desirable benefits of an erosion-resistant turbine gas path seal. A high-temperature erosion test rig designed by Lewis personnel will be used to evaluate present state-of-the-art sealing systems. Present test rig capabilities allow combustion temperatures of 2800° F and particulate velocities of about 800 ft/sec. Erosion variables can be repeated accurately to provide representative

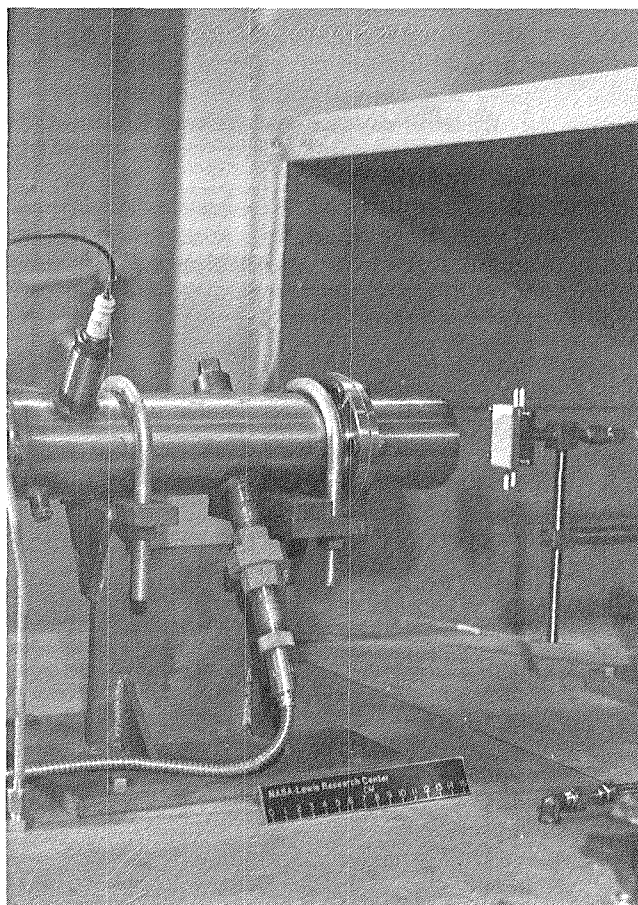


Gallium arsenide phototransistors (magnified)

erosion data for many sealing systems. The data generated during this testing should provide insight into the high-temperature erosion process for gas path seals. From the empirical studies of various sealing systems, analytical tools for the prediction of erosion resistance should be developed and should lead to improved gas path seals.

### Spiral-Groove Face Seal Film Thickness

Noncontacting (spiral groove) face seals control face separation and thus extend shaft seal life and operating speed without compromising leakage. The spiral-groove face seal is similar in construction to a conventional face seal except that a self-acting gas bearing geometry in the form of spiral grooves is machined on one of the two sealing faces. When the shaft rotates, the spiral grooves act to pump fluid between the sealing faces and separate them by a slight



High-temperature particulate erosion rig

amount (approx 0.0002 in.), thereby permitting the seal to operate in a noncontacting mode. An experimental investigation of film thickness measurement for a spiral-groove face seal was performed at Lewis. The objective was to obtain film thickness as a function of shaft speed for a face seal operating in air at ambient conditions.

A comparison between the experimental results and a mathematical model for predicting film thickness gave the following significant results: (1) Current analyses overpredicted the measured film thickness at lower speeds and underpredicted the measured film thickness at higher speeds; (2) the film thickness was unsteady (i.e., vibratory in nature); and (3) the spiral-groove geometry was capable of maintaining seal face separation without contact even under vibratory conditions.

### Lower Cobalt Content in Superalloy

Cobalt, one of the strategic elements in short supply in the United States, is widely used in gas turbine engine applications. Ninety percent of the cobalt used in the United States is imported and comes mainly from countries that in critical times may not remain reliable suppliers. Interruption of cobalt imports could then seriously disrupt our commercial and military aviation, as no substitutes have been developed. In some applications, such as an alloy used for gas turbine engine disks, test results suggest that nickel can be substituted for cobalt. Nickel was incrementally

substituted for the normal cobalt content of 17 percent in Udimet-700, a typical nickel-base superalloy. By proper selection of heat-treating conditions, the stress-rupture lives of powder-metallurgy-processed alloys increased substantially as cobalt was reduced from 17 percent to 4.3 percent. These results suggest that the stress-rupture life of Udimet-700 can be improved while substantially reducing the amount of cobalt in the alloy. For creep-rate-controlled applications, however, further alloy modifications are needed since creep rate increased as cobalt was reduced in the alloy.

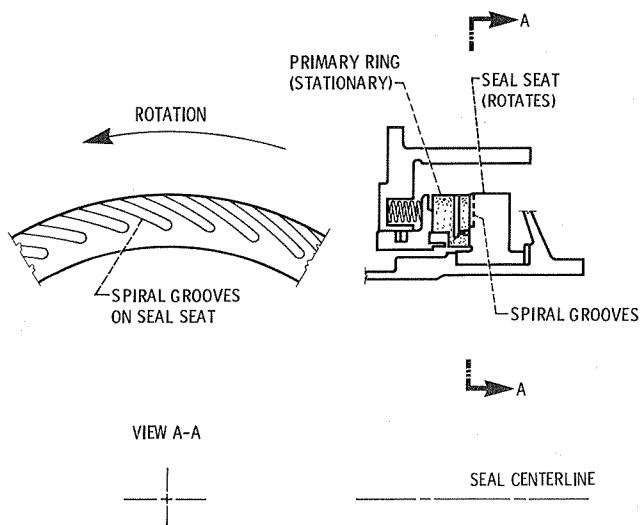
### Corrosion-Resistant Bearing Steels

Corrosion is responsible for many bearing rejections during overhaul of U.S. Navy and Air Force aircraft systems. Use of corrosion-resistant steels will significantly reduce bearing rejection. AMS 5749 and AMS 5900 are steel alloys developed for high hardenability and corrosion resistance. Their use for critical aerospace rolling-element bearing applications is being investigated. Testing in NASA five-ball fatigue testers shows that the rolling-element fatigue lives of these materials are up to eight times that of the standard aircraft turbine engine mainshaft bearing material, AISI M-50. In corrosion tests designed to simulate the mechanism of corrosion found in rejected aircraft turbine engine bearings, AMS 5749 proved to have significantly better corrosion resistance than AISI M-50.

Currently, AISI 440C is used for bearings in cryogenic turbopumps such as in the space shuttle main engines. Corrosion resistance, high hardness, and long fatigue life are requirements for current and future turbopump bearings. AMS 5749 and 5900 appear to be promising materials for this application as well as for turbine engine mainshaft bearings.

### Applications of PMR-15 Polyimide Composites

One of the rewarding aspects of the Lewis PMR polyimide development has been the successful demonstration of PMR-15 polyimide composite materials as viable engineering materials. A number of materials based on PMR-15 have been commercially available from the major suppliers of composite materials since the mid-1970's. Because of their commercial availability, processibility, and excellent retention of properties at high temperatures, PMR-15 composites have been used to fabricate a variety



*Spiral-groove face seal*

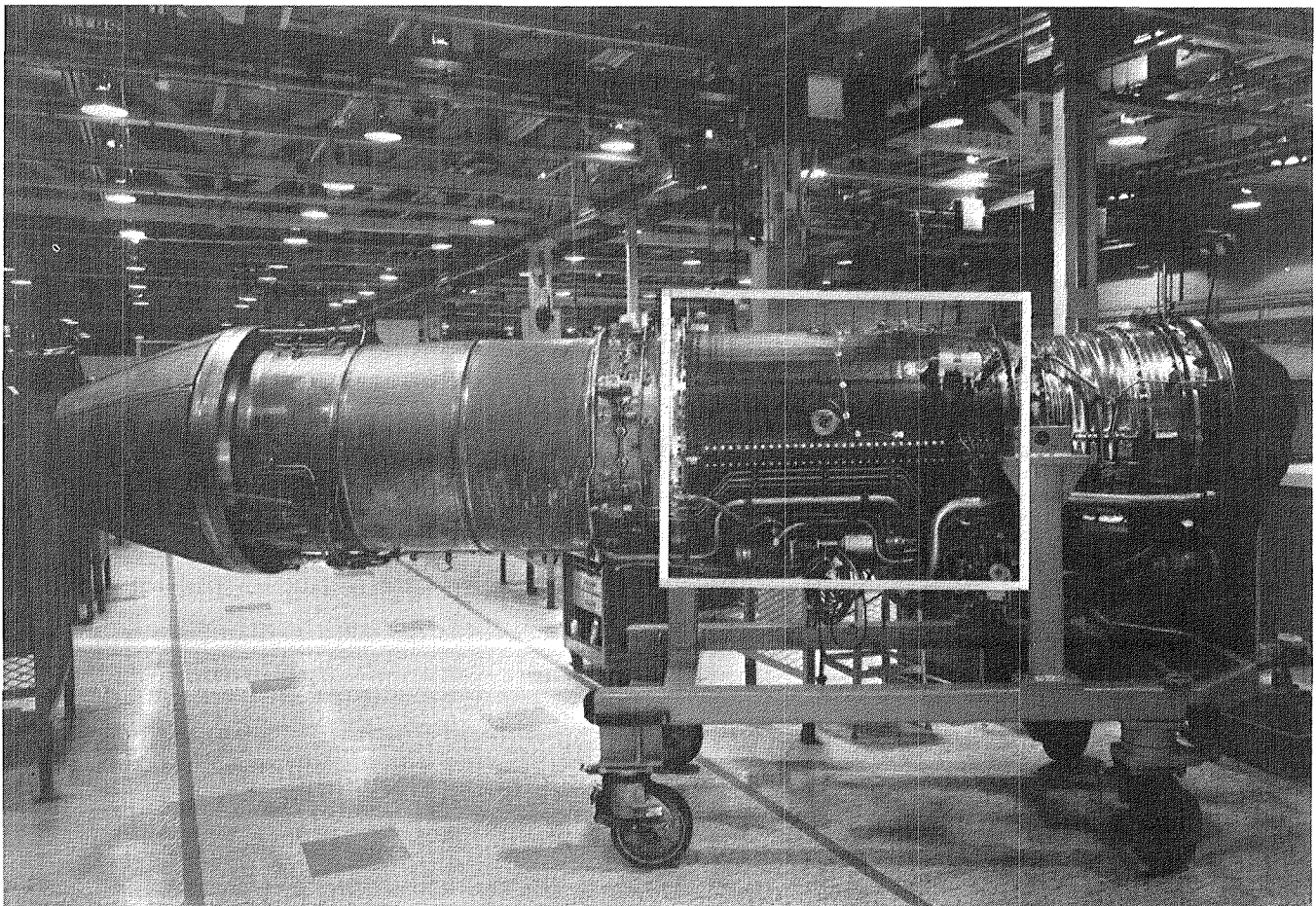


of structural components. These components range from small compression-molded bearings to large autoclave-molded aircraft engine cowls and ducts. Processing technology and baseline materials data are being developed for the application of PMR-15 composites in aircraft engines, space structures, and weapon systems. An example of the use of PMR-15 polyimide composites in engines is the outer duct of the F404 engine. The graphite fiber/PMR-15 composite duct is being developed by the General Electric Co., under a program jointly sponsored by the U.S. Navy and NASA, as a replacement for the current bill-of-materials titanium duct. The composite duct has successfully withstood over 1000 accelerated mission test cycles during a total engine exposure time of 700 hr. The graphite

fiber/PMR-15 polyimide composite duct is scheduled to be introduced into production in 1985.

#### **Ultrasonic Verification of Low-Carbon-Steel Toughness**

Substantial cost savings can be realized by having rapid, nondestructive methods for monitoring and verifying mechanical properties of materials that are usually subjected to destructive testing procedures for determining strength, toughness, etc. Therefore, upon a request received from an interested firm, a feasibility study was conducted at Lewis to determine whether ultrasonic measurements could be used to rank commercially produced steel plates according to fracture toughness. Three heats of a low-carbon steel were subjected to drop weight

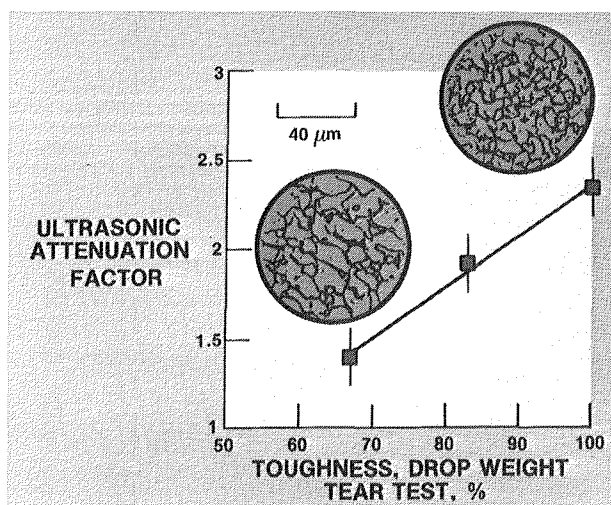


*Graphite fiber/PMR-15 polyimide outer duct on F404 engine*

tear testing (DWTT). The plates exhibited a range of DWTT toughness values corresponding to the heats. Then a Lewis-developed pulse-echo ultrasonic measurement technique was applied, and an ultrasonic attenuation factor was calculated for specimens from each heat. A strong linear correlation was found between the ultrasonic factor and DWTT toughness value. Photomicrographs of the two extreme heats show the influence of grain size: as grain size decreases, the toughness and ultrasonic factor increase. The nondestructive, ultrasonic testing method is a promising alternative to the DWTT method, which is expensive and time consuming. The ultrasonic method could provide prompt feedback control of processing parameters and certification of the material properties of finished products.

### Prediction of Thermal Strength Degradation of Boron-Aluminum Composites

During the fabrication and high-temperature use of boron-aluminum composites, a reaction can occur between the boron fibers and the aluminum matrix. If the reaction product exceeds a certain critical thickness, a degradation of fiber strength occurs and results in a general loss of composite strength. From a study of the factors that influence this reaction-controlled strength degradation, a fiber fracture model was developed to predict the onset and severity of the degradation.



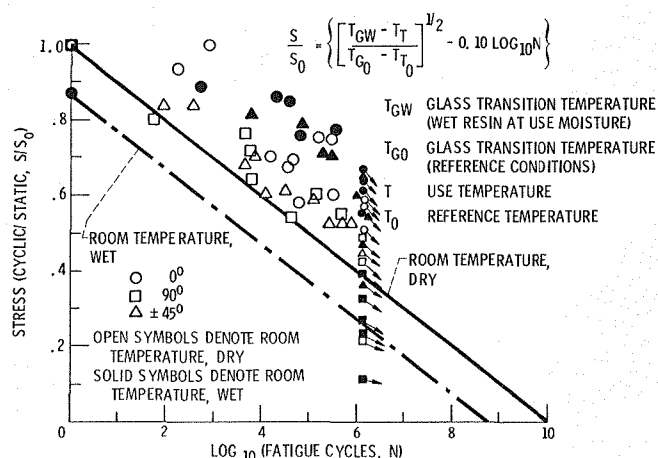
*Influence of grain size on ultrasonic attenuation factor and toughness*

The model assumes a parabolic time-dependent growth of the reaction product and Griffith fiber fracture initiated by cracks across the reaction product thickness. The model accurately predicts the effects of time, temperature, and original fiber surface condition on fiber strength. Other factors, such as fiber diameter and aluminum alloy composition, were found to have negligible effects on reaction-controlled fracture.

### Durability and Life of Fiber Composites

A major concern in the fiber composites community over the last 10 years has been an accurate prediction, or even a good approximation, of the durability and life of fiber composite components or structures in service environments. Service environments of major concern are temperature, moisture, mechanical loads (static and cyclic), and various combinations of these, or more concisely "hygrothermomechanical" (HGTm) environments. In response to this concern, research efforts at Lewis are directed toward developing the methodology required to predict the life or durability of composite structural components in turbine jet engine service environments. A part of this research effort has been to develop predictively correct models for determining the hygrothermomechanical degradation of composite strength (durability and life). The predictively correct models sought are first derived empirically by using statistical methods and available HGTm data.

Statistical analysis (least-squares method and multiple regression) was used to determine and



*Compressive life and durability*

---

quantify the significance of HGTM variables on composite tensile strength (durability and life) of boron/epoxy (B/E) and high-modulus-graphite/epoxy (HMG/E) composites. The multiple regression analysis reduced the number of HGTM variables from the 15 assumed in the initial curve-fit model to 6 or less. The predicted results, using 6 coefficients, agreed with those using 15 coefficients within 0.1 percent. Predictive models derived for the tensile durability and life were used in conjunction with assumed isoparametric relationships to derive predictive models for the compression and shear durability and life of B/E and HMG/E composites. A "generalized" predictive model was derived for the durability and life of graphite-fiber/resin-matrix composites to be used mainly in preliminary designs. The generalized predictive model is of simple form and predicts values that are conservative when compared with available measured data.

### **Compression Behavior of Unidirectional Composites**

The flexural test (three-point bend), which is used extensively for quality control of composites, subjects a test specimen to both longitudinal tension and compression as well as interlaminar shear. Both the flexural strength and longitudinal tension strength can be determined more easily than the longitudinal compression strength. It seems appropriate then to investigate the possibility of determining the longitudinal compression strength of unidirectional composites by using longitudinal tensile strength and flexural strength test data for the same composite system.

A recent investigation was completed at Lewis wherein the longitudinal compression behavior of unidirectional fibrous graphite/epoxy composites was studied. The Illinois Institute of Technology Research Institute (IITRI) test method was used to test thick and thin test specimens. The test data were interpreted by using the stress-strain curves from back-to-back strain gages, examination of fracture surfaces by scanning electron microscope, and predictive equations for distinct failure modes including fiber compression failure, Euler buckling, delamination, and flexure. The results show that the longitudinal compression fracture is a tiered combination of delamination, flexure, and fiber breaks. No distinct fracture surface characteristics could be associated with unique failure modes. An equation was developed that can be used to determine the longitudinal

compression strength from the longitudinal and flexural strengths of the same composite system

### **Structural Dynamic Simulation of Rotor-Bearing-Stator System**

Simulations of rotor-squeeze-film bearing-stator systems are inherently nonlinear because of (1) the inherent behavior characteristic of squeeze films, particularly during transient conditions, and (2) potential structural interactions wherein either large deformation kinematics or material nonlinearity (plasticity) is excited.

Because of such features, the overall rotor-bearing-stator simulation must be able to incorporate the various sources of nonlinearity. Additionally, to enable efficient solutions in situations wherein various model components are linear, the overall simulation scheme must incorporate substructuring capabilities. Furthermore, since transient problems need to be considered, such features must be accommodated by the various integration algorithms used to solve the governing model equations.

A general-purpose squeeze-film-damper/interactive-force finite element has been developed at the University of Akron under a grant from Lewis. This finite element was implanted in a general-purpose finite element computer code. Three numerical integration methods were incorporated as part of the implantation in order to solve the governing structural dynamics equations of the interactive finite element. The general-purpose code was then used to predict the structural dynamic response of the rotor-stator-coupled structure subjected to unbalance and impulse excitations. The structural dynamic responses predicted include (1) bearing-rotor trajectories, (2) stator trajectory, (3) rotor orbit, and (4) force, velocity, and acceleration histories at a given location in the coupled structure. Three-dimensional postprocessors have been developed to graphically display the voluminous predicted results in isometric views.

### **Double Linear Damage Rule for Fatigue**

The double linear damage rule (DLDR), developed jointly by Lewis and Case Western Reserve University under a grant from Lewis, permits accurate assessment of the nonlinear accumulation of fatigue crack initiation damage resulting from variable-amplitude loading histories of structural components. Simple,

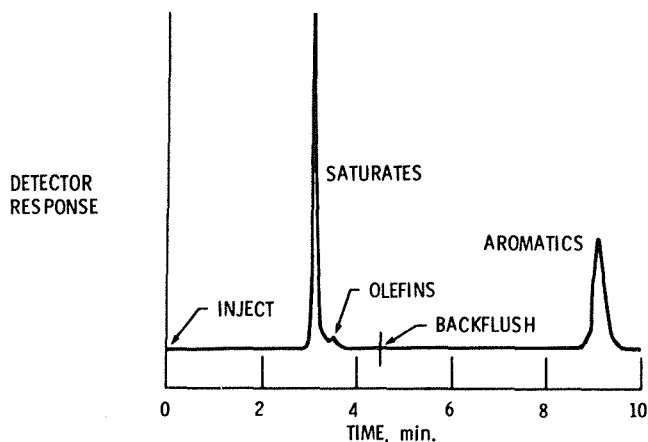
verified procedures have been developed to apply to the difficult problem just described. The DLDR replaces the conventional Miner linear damage rule. The DLDR requires no more information than does the Miner rule but is more accurate because the Miner rule assumes linearity and the DLDR accounts for nonlinearity. The extent of nonlinearity becomes especially crucial when structures are subjected to both low-cycle and high-cycle fatigue loadings.

The DLDR is a concept arrived at through viewing the fatigue process as two sequential phases: phase I, associated with microscopic changes in the surface layer of the material being fatigued, and phase II, with the propagation of microcracks to the point that is classified as fatigue crack initiation on the macroscopic engineering level.

The application of the newly proposed rule involves two steps, each similar to the conventional application of the classical Miner rule. When the sum of the cycle ratios based on phase I lives reaches unity, phase I is presumed to be complete, and further loadings are summed as cycle ratios based on phase II lives. Once phase II cycle ratios sum to unity, failure by macrocrack initiation is presumed to occur. No physical properties or material constants other than those normally required in a conventional Miner rule analysis are required for application of the DLDR.

### Improved Method for Hydrocarbon Analysis

The levels of various hydrocarbon classes or types present in aircraft fuels are extremely



*Liquid chromatographic analysis of fuels*

important in understanding and predicting engine performance. Aromatics, saturates, and olefins are typically determined by using standard chromatographic methods, that are time consuming, limited in latitude, and subject to a number of fundamental errors. High-performance liquid chromatography has been employed as an improved technique but is limited by problems in obtaining suitable calibration standards and in accurately determining low quantities of olefins. Research conducted at Lewis has resulted in an improved method that uses the liquid chromatograph. This method incorporates a fast, simple scheme for preparing the aromatics calibration standard that requires no information on the source of the fuel. A portion of the fuel sample is reacted with sulfuric acid to provide a chemically modified version of the fuel that serves as the standard. The olefins determination is limited by interference from the saturates peak, which is located in close proximity to the olefin peak in the chromatogram. In the improved method, a substantial portion of the interfering saturates is removed by diverting this fraction out of the system (backflushing) while preserving the olefin band intact. This simple, but effective, extension of the conventional method permits accurate determinations of olefin content to levels as low as 0.3 vol %.

### Planetary Gear Dynamic Load Analysis

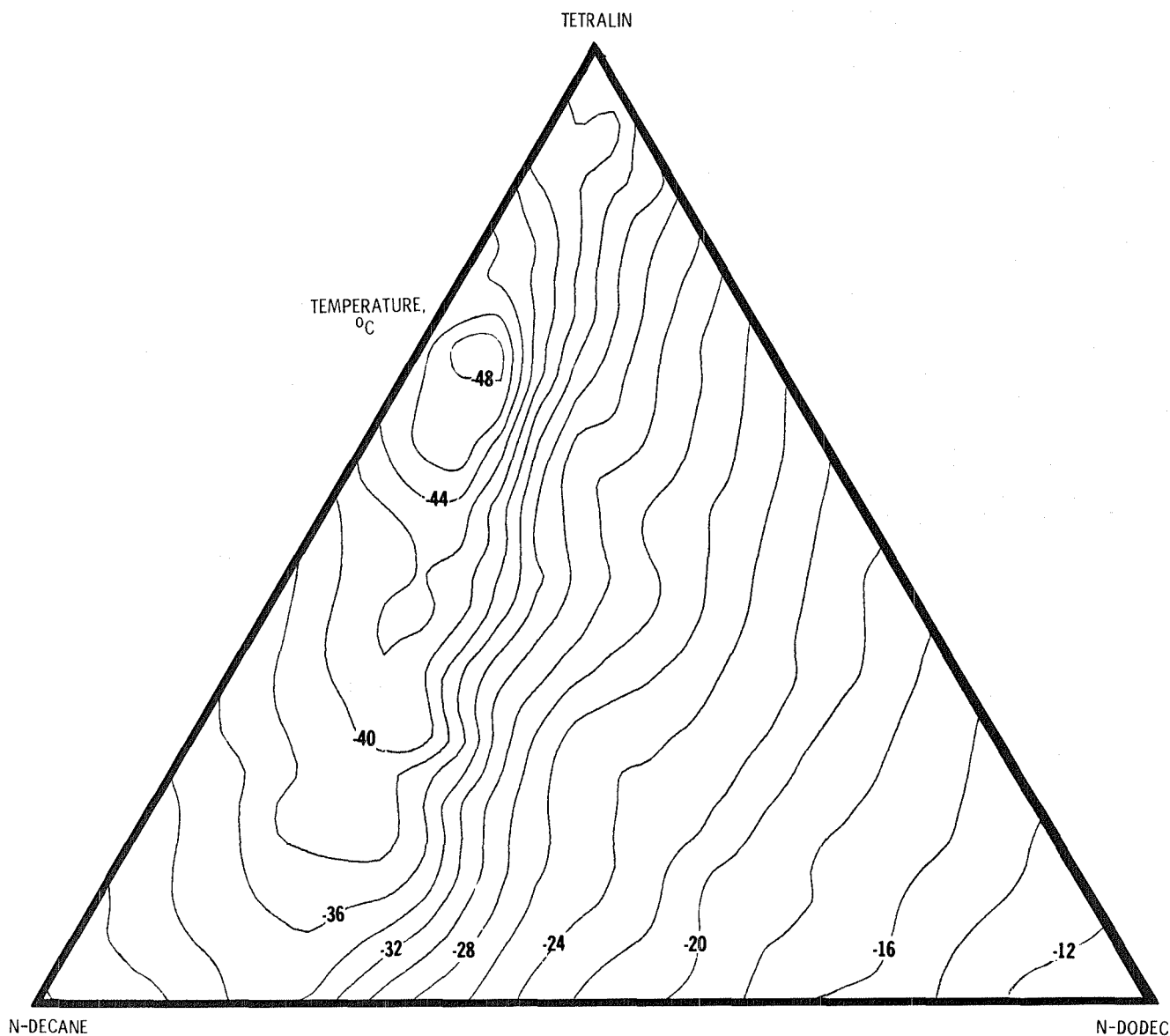
Under contract to Lewis, the Hamilton Standard Division of United Technologies Corp. has developed a dynamic load stress and deflection analysis for a planetary gear system. The computer program determines the dynamic loads, stresses, deflections, and pressure-volume factor for a planetary gear system with up to 20 planets. The program can use standard or high-contact-ratio spur gears and determines the various stresses, etc., for the sun-planet and ring-planet meshes. Various gear profile modifications, tooth errors, gear masses, and damping coefficients can be used in the program. The program also plots the different output parameters for a single tooth or for 8 teeth in series passing through the mesh.

### Hydrocarbon Solid-Liquid Phase Equilibria

Hydrocarbon fuels are mixtures of many chemical species and exhibit complex freezing and melting behavior. To understand and predict

this behavior, it is essential to understand the behavior of simpler mixtures containing two or three species. Differential scanning calorimetry has proven to be a rapid and accurate technique for measuring energy loss or gain and thus determining liquid-solid phase diagrams for several binary and two ternary hydrocarbon systems. In addition to the freezing or melting points, the technique determines the heats of fusion of the mixtures and the formation of

eutectics and solid solutions. The melting-point isotherms for the ternary system tetralin-decane-dodecane are shown in the central region of the accompanying diagram. This mixture is a reasonable model for real jet fuels that exhibit freezing points and contain proportions of saturated and aromatic hydrocarbons. These isotherms provide the thermodynamic data necessary for a predictive model of real fuel freezing behavior.



Freezing-point isotherms for ternary hydrocarbon mixture

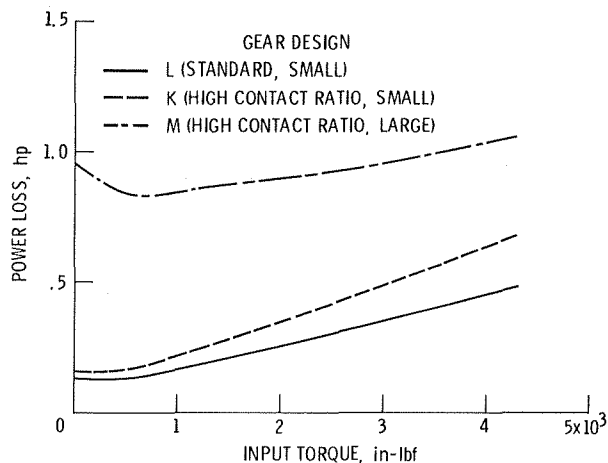


## Prediction of Power Loss in Nonstandard Spur Gears

Spur gears with nonstandard tooth proportions are often stronger and quieter than conventional gears; however, these advantages are often offset by higher power loss. Most existing power loss prediction methods are intended to provide an estimate of full-load power loss for gears of standard proportions. A new method developed at Lewis provides a technique for calculating standard gear losses over a broad range of gear geometry and operating conditions. This method has now been extended to allow power loss predictions to be made for nonstandard external and internal spur gears.

High-contact-ratio gearing (gears having more than one tooth in contact) is of current interest for helicopter transmission systems. These nonstandard gears have the potential of higher load capacity as well as quieter operation. A possible drawback of these gears is that they can be less efficient than their standard gear counterparts. The new power-loss prediction method will allow the gear designer to predict and improve the performance of high-contact-ratio gears through the proper selection of geometry.

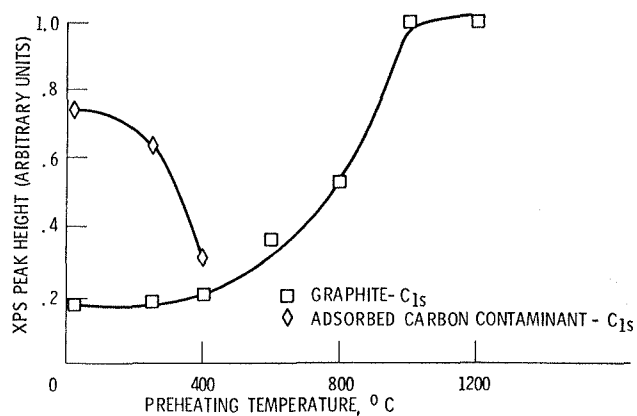
Power loss is predicted for three gears designed for the same application. Gear L is a standard gear; gears K and M are both high-contact-ratio gears, but of different size. From the analysis based on gear design K, it is possible to design a high-contact-ratio gearset with an efficiency comparable to that of a standard gear design.



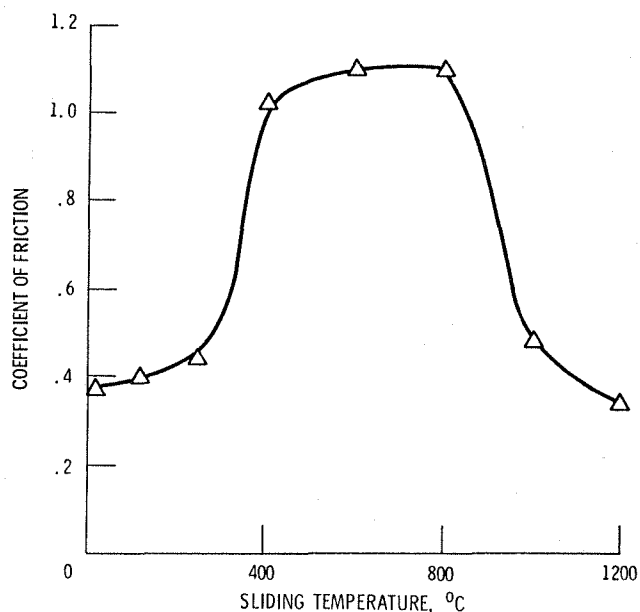
Power loss prediction of standard and high-contact-ratio spur gears

## Tribological Properties of Silicon Carbide

Experimental chemical analyses, X-ray photoelectron spectroscopy (XPS), depth profiling, and friction studies have been conducted on silicon carbide surfaces. The work has been performed in vacuum and in argon. Both sintered polycrystalline and single-crystal materials were studied. The studies reveal that at temperatures of 1000° C, both materials graphitize and thus markedly decrease friction.

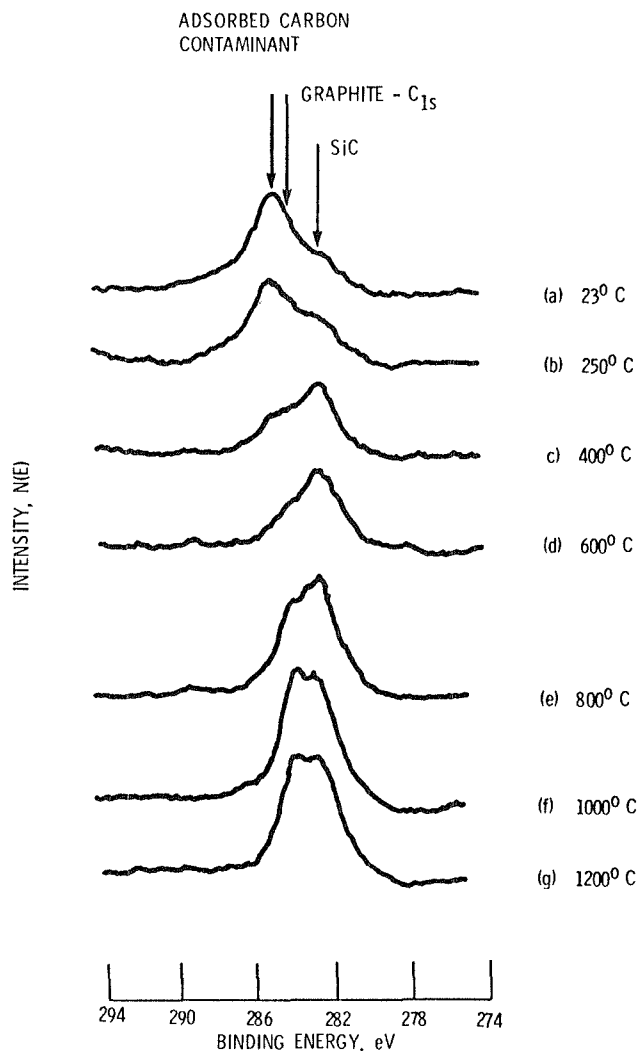


Peak heights on sintered polycrystalline SiC surface preheated to 1200° C



Contact of rough surfaces

Photoelastic emission lines of silicon carbide reveal three distinguishable peaks associated with (1) adsorbed carbon contaminant, (2) graphite, and (3) silicon carbide. Above 600° C, the SiC peak is split. XPS peak heights of the adsorbed carbon contaminant and the graphite reveal that as temperature increases, carbon contaminant decreases and graphite increases. Above 1000° C, the entire surface is covered with a graphite layer. The rapid decrease in coefficient of friction of sintered SiC in contact with iron above 800° C correlates well with the graphitization of the surface.



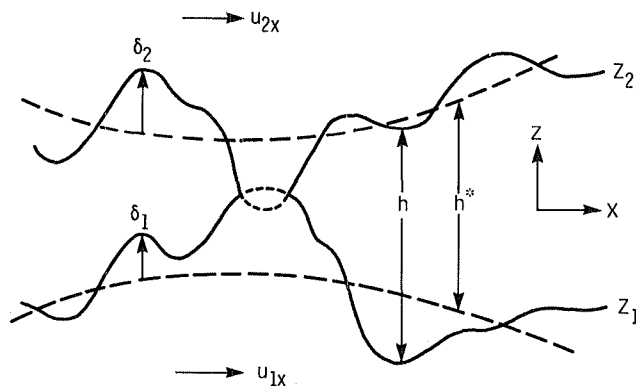
Effect of temperature on coefficient of friction for sintered polycrystalline SiC surface sliding against iron rider

## Real Surface Effects in Hydrodynamic Lubrication

The Reynolds flow equation has been cast into a new form that is applicable to randomly rough surfaces in two dimensions. The solution of the equation yields the statistically averaged pressure across the nominal thickness of a lubricant film. The averaging is performed on the solution, rather than being incorporated as an assumption in deriving the equation. The method used is a variation of the Green function technique, which is a standard method in statistical physics. This is its first use within this context. The textures on each surface, together with any interrelation between them, are described by two two-point correlation functions. Only two parameters are involved—the ratio of rms roughness to film thickness and the aspect ratio of a typical surface feature. The parameters are incorporated into two flow factors: one describing the effect of pressure gradient and the other describing the effect of surface texture. These flow factors are then applied to the Reynolds equation.

Flow factors have been obtained for a range of aspect ratios of surface features, between the extremes of longitudinal and transverse ridges. The factors have also been obtained for a range of roughness height to about half of the film thickness. Beyond that limit, extensive mechanical contact begins and the statistical model is no longer valid. Within the region of validity, the results compare favorably with earlier computer simulation.

The theory may be applied to a greater variety of surface textures by the derivation of higher-order correlation functions.



Contact of rough surfaces

---

Title	Lewis contact	Phone number, (216) 433-4000, extension	Headquarters program office
Microwave Ice Accretion Meter	Robert F. Ide	5166	OAST
Energy Efficient Engine	Carl C. Ciepluch	6644	OAST
Combustion Systems for Broadened-Property Fuels	James S. Fear	6158	OAST
Three-Dimensional Compressible Flow Analysis for Propellers	Lawrence J. Bober	5520	OAST
New Flow Visualization Technique	George L. Stefko	738	OAST
Cascade and Sweep Effects on Advanced Turboprop Flutter	Robert E. Kielb	5104	OAST
Flow-Field Measurements in a Transonic Fan Stage	Anthony J. Strazisar	6846	OAST
Bird Impact Analysis Package for Turbine Engine Fan Blades	Murray S. Hirschbein	272	OAST
Finite Element Simulation of Turbofan Noise	Kenneth J. Baumeister	220	OAST
Catalytic Combustors for Gas Turbine Engines	Andrew J. Szanislo	6158	OAST
Combustor Liner Cooling Technology	Carl T. Norgren	268	OAST
Primary Zone of Small Gas Turbine Combustor	Daniel C. Briehl	208	OAST
Turbine Bypass Concept	Leo C. Franciscus	6183	OAST
Nonlinear Structural Analysis of Propellers	Robert A. Aiello	272	OAST
Reproducible Growth of Single- Crystal Silicon Carbide	J. Anthony Powell	353	OAST
Optical Probe for Turbine Engine Blade Vibrations	Louis J. Kiraly	6950	OAST
Turbine Engine Rotor Computer Code	Albert F. Kascak	6975	OAST
Simulations of Temperature Disturbances on Turbine Engines	Willis M. Braithewaite	5502	OAST
High-Speed Balancing of Turbine Engines	David P. Fleming	6975	OAST
Advanced Rotary Telemetry System	Daniel J. Lesco	350	OAST
Turbomachinery Panel Method	Eric R. McFarland	6847	OAST
Line-of-Sight Laser Anemometer	Richard G. Seasholtz	353	OAST
Holographic Motion Pictures	Arthur J. Decker	353	OAST
Flow Visualization of Turbulent Coaxial-Jet Mixing	Cecil J. Marek	6903	OAST
Internal Flow in an Internal Combustion Engine	Harold J. Schock	6942	OAST
High-Temperature Photoswitch	Robert J. Baumbick	6136	OAST
High-Temperature Particulate Erosion Rig	Robert F. Handschuh	6895	OAST
Lower Cobalt Content in Superalloy	Fredric H. Harf	6162	OAST
Spiral-Groove Face Seal Film Thickness	Eliseo DiRusso	6895	OAST
Corrosion-Resistant Bearing Steels	Richard J. Parker	6101	OAST
Application of PMR-15 Polyimide Composites	Tito T. Serafini	6179	OAST
Ultrasonic Verification of Low- Carbon-Steel Toughness	David R. Hull	6107	OAST

---

<b>Title</b>	<b>Lewis contact</b>	<b>Phone number, (216) 433-4000, extension</b>	<b>Headquarters program office</b>
Prediction of Thermal Strength Degradation of Boron-Aluminum Composites	James A. DiCarlo	6602	OAST
Durability and Life of Fiber Composites	Christos C. Chamis	6831	OAST
Compression Behavior of Unidirectional Composites	Christos C. Chamis	6831	OAST
Structural Dynamic Simulation of Rotor-Bearing-Stator System	Christos C. Chamis	6831	OAST
Double Linear Damage Rule for Fatigue	Gary R. Halford	6852	OAST
Improved Method for Hydro- Carbon Analysis	Gary T. Seng	6815	OAST
Planetary Gear Dynamic Load Analysis	Dennis P. Townsend	6101	OAST
Hydrocarbon Solid-Liquid Phase Equilibria	Frank J. Zeleznik	5210	OAST
Prediction of Power Loss in Nonstandard Spur Gears	Neil E. Anderson	6101	OAST
Tribological Properties of Silicon Carbide	Kazuhisa Miyoshi	5271	RTM
Real Surface Effects of Hydrodynamic Lubrication	Bernard J. Hamrock	6151	RTM

# Space

## Propulsion

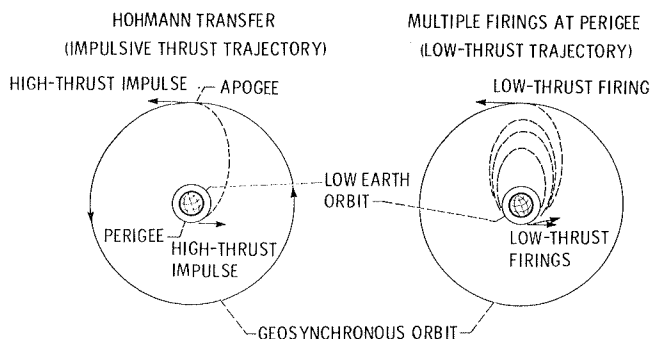
### Low-Thrust Orbit Transfer

Future space missions will deploy or build large space structures in low Earth orbit and then transfer them to their operational location in geosynchronous orbit. The conventional Hohmann transfer, which requires minimum propellant, uses a high-thrust impulse to send the spacecraft into an intermediate elliptical orbit with apogee at geosynchronous altitude. At apogee, a second impulsive engine burn circularizes the trajectory into the desired geosynchronous orbit. However, the large, lightweight space structures planned are incapable of safely withstanding the large forces imposed by the high-thrust Hohmann transfer.

An alternative approach to the Hohmann transfer has been designed. Multiple low-thrust engine firings at perigee move the spacecraft into successive elliptical orbits, each with a higher apogee, until the desired altitude is reached and the orbit is then circularized. The low-thrust trajectories keep the structural loads within the spacecraft limits.

### Low-Thrust Chemical Rocket Engines

Low-thrust chemical propulsion is being considered for transferring acceleration-limited large space systems from low Earth orbit to geosynchronous equatorial or other high orbits. To aid in identifying and assessing the potential of various rocket engines for application to low-thrust propulsion systems, study contracts were awarded to evaluate the theoretical performance of various propellant systems, to establish the chamber pressure and thrust limits of

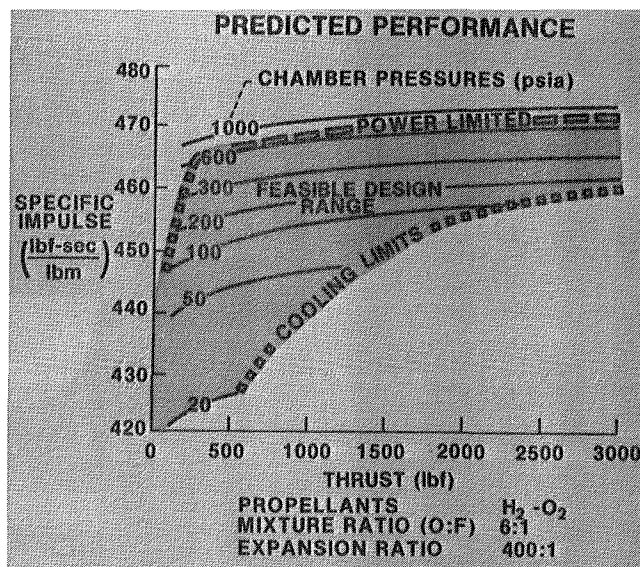


Low-thrust orbit transfer

conventional regenerative cooling, to establish cycle power requirements, and to identify technology requirements. The study included propellant combinations of oxygen with hydrogen, methane, and RP-1 for thrusts from 100 to 3000 lb and chamber pressures from 20 to 1000 psia. Methane and hydrogen regenerative cooling were found to be viable candidates, with hydrogen providing the largest low-thrust, design-point operating envelope. Results of performance, cycle power, weight, and complexity analyses on a matrix of 17 engine systems showed the hydrogen-oxygen expander cycle to have the highest relative merit rating. Identified enabling technologies included prediction and verification of pump and thrust chamber performance, ignitor miniaturization, and component operating life demonstration.

### Simplified Prediction of Thrust Chamber Life

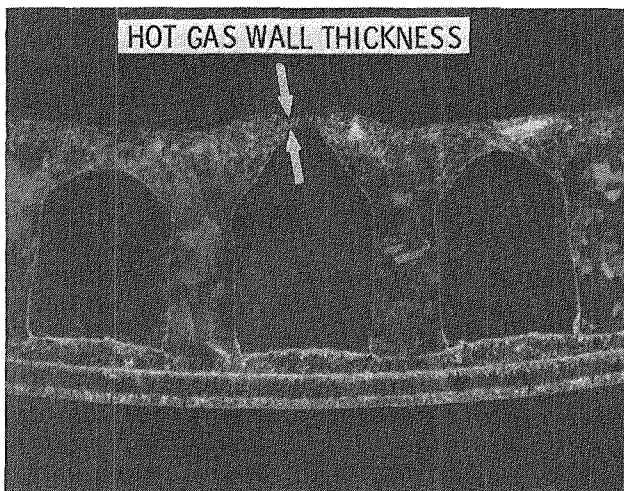
The reusability requirement of the space shuttle main engine (SSME) introduced the need for life prediction of rocket thrust chambers. Life predictions of SSME type, regeneratively cooled, milled-channel thrust chambers have been based on low-cycle-fatigue principles. Thrust chamber tests, however, have indicated that the coolant channel walls in the failed areas progressively bulge and thin during cyclic firing. Failure



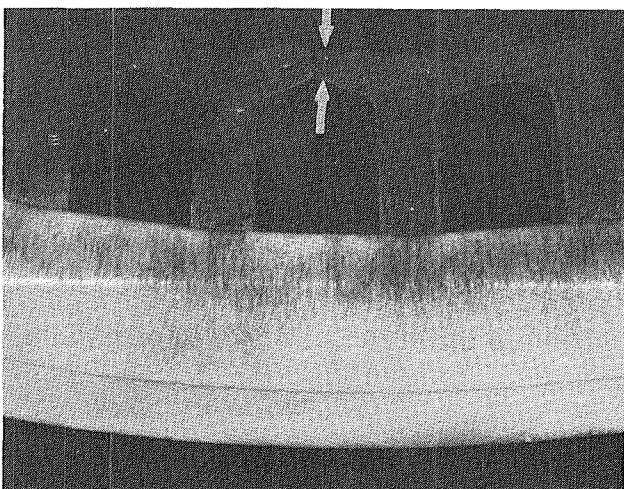
Predicted performance of expander cycle as low-thrust chemical rocket engine



analyses have indicated that ductile rupture can be a more limiting mode of failure than fatigue failure. The mechanism of coolant-channel-wall incremental distortion and thinning can be investigated by finite-element inelastic analyses. Because these analyses are time consuming and difficult to perform, they are not practical for evaluating the effects of changing various design parameters. A simplified life prediction procedure that includes ductile rupture in addition to fatigue damage has been developed to allow preliminary evaluations prior to detailed analyses.



(a) OFHC copper thrust chamber.



(b) Narloy-Z thrust chamber.

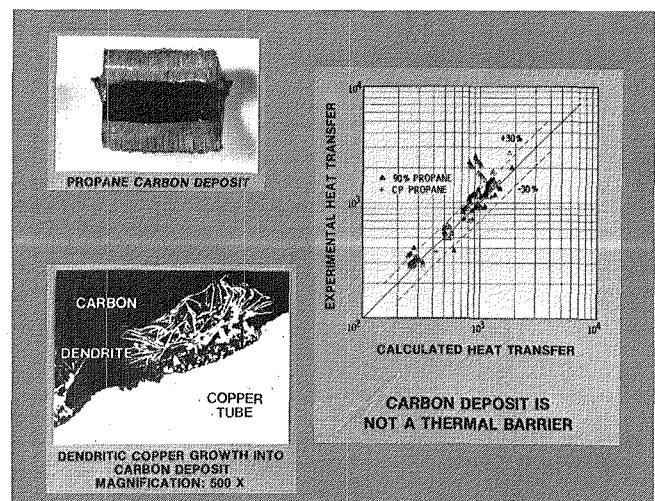
*Cross-sectional views of thrust chamber failure sites*

Simplified analysis results predicted a coolant wall thinout rate that compared favorably with that resulting from short, cyclical test firings of experimental chambers at Lewis. Simplified analyses also indicated that ductile rupture is the dominant failure mode for thrust chambers of OFHC (oxygen-free high conductivity) copper and that fatigue interacting with coolant wall thinning is the failure mode for thrust chambers with liners of stronger copper alloys. This was also in general agreement with the test results.

Because the chambers for which the analyses were performed were test fired for short durations, the analyses did not include time-dependent creep effects such as creep ratcheting. For actual rocket engines, where the firing cycle is considerably longer than the test cycle, creep effects must be accounted for, along with plastic ratcheting and low-cycle fatigue. Follow-on development work includes creep effects in the simplified procedure.

### Cooling with Hydrocarbon Fuels

Several hydrocarbon fuels are being considered for future liquid-fueled rocket boosters. Heat transfer tests were conducted by flowing different hydrocarbon fuels through an instrumented, heated tube. Wall temperatures, flow velocities, and materials were typical of rocket regenerative cooling applications. Postrun analysis showed that carbon deposition rates were 50 percent higher with propane than with RP-1, the conventional fuel used for booster engines. This precipitated an early shift in interest away from

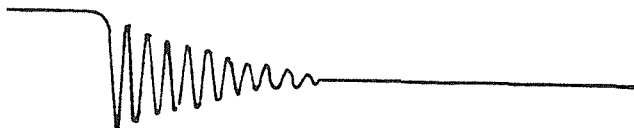


*Propane heat transfer correlation*

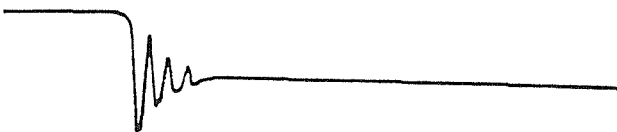
propane as a potential fuel. However, later thermal analysis showed that a propane heat transfer correlation was applicable even in the presence of coking and that the amount of carbon deposited did not represent a significant thermal resistance. The availability of these data and a substantiating model should prompt a renewed consideration of propane as a potential fuel for boosters.

### Eddy-Current Damping for Rotating Machinery

The high-speed rotors of many lightweight turbomachines can experience large-amplitude vibrations. These vibrations can damage both bearings and seals and thus result in operation at reduced power or, in some instances, complete shutdown. Conventional methods of controlling vibrations, such as viscous oil or elastomeric dampers, have reduced effectiveness in extreme environments such as the very low temperatures encountered in cryogenic turbopumps. Another method of controlling vibrations is known as magnetic or eddy-current damping. Current flow induced in a conducting material when vibrating in a magnetic field produces forces that oppose the motion. These forces are significantly greater when the conductor operates in a low-temperature environment. This makes eddy-current damping ideally suited for use in cryogenic turbomachinery, and with further development such dampers can find application



VIBRATING RESPONSE IN AIR AT ROOM TEMPERATURE (20° C)



VIBRATING RESPONSE IN LIQUID NITROGEN AT -195° C

*Comparative results of eddy-current damping*

in many other types of rotating systems.

Preliminary tests were conducted on a free-vibrating beam apparatus. The accompanying traces show the response of a free-vibrating beam that is attached to a copper conductor. The conductor is made to vibrate between the pole faces of a permanent magnet. The measured damping force is approximately three times greater in liquid nitrogen (—195° C) than in air (20° C).

For use in the space shuttle main engine liquid-oxygen turbopumps, the damper assembly consists of a number of high-energy permanent magnets located circumferentially around the bearing support. High-purity copper conductors attached to the outer races of the ball bearings with squirrel-cage springs vibrate between the pole faces of the magnets. Eddy currents are generated in the conductors and produce forces opposing rotor precessional motion.

### Improved Ion Thruster Performance

Two important factors in total propulsion system efficiency are the power required to produce ions for electrostatic thrusters and propellant efficiency. A new magnetic containment circuit composed of ring cusps was developed and optimized. The concept reduces the number of ions that are lost to the walls of the discharge chamber and thus greatly improves performance. With argon propellant, for example, the lower ion beam production cost results in a power saving of about 30 percent over conventional ion thrusters. This power saving translates into large reductions in thruster system cost, weight, and thrusting time and also into improved payload capability.

### Ion Auxiliary Propulsion System

The ion auxiliary propulsion system (IAPS) flight hardware completed its development and test program and was delivered to the spacecraft contractor for integration with the Air Force satellite on which it will fly. The IAPS consists of two modules, each containing a thruster subsystem and elements of a diagnostic subsystem.

The thruster subsystem comprises a thruster-gimbal-beam shield unit, a power electronics unit, a digital controller-interface unit, and a propellant system. The diagnostic subsystem has instrumentation to measure particle deposition, to detect charged particles, and to measure the

voltage difference between thruster ground and space plasma.

All flight hardware successfully completed flight qualification tests as components and in systems. Further tests will be conducted on the spacecraft prior to launch. The IAPS was developed and tested by the Hughes Aircraft Co. under contract to Lewis. Tests in support of the flight are continuing at Lewis.

### **Rapid Measurement of Sputter Erosion**

Plasma discharges are of fundamental importance to many disciplines, including space propulsion. All materials exposed to plasma discharges experience some degree of erosion (sputtering) due to bombardment by ions from the discharge. Knowledge of the sputtering rates is frequently essential in the design and operation of plasma systems. For example, electron bombardment ion thrusters require long lifetimes of 15,000 hours or more for many missions. In the past, long, costly tests were conducted to determine the sputtering rates of various discharge chamber surfaces. A technique was needed for quick, accurate measurement of sputter erosion rates.

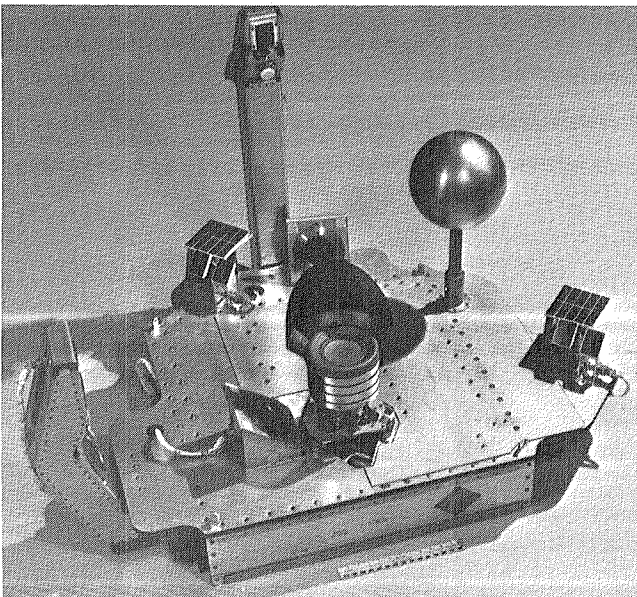
Hughes Research Laboratories, under contract to Lewis, investigated rapid erosion measurement

techniques. The surfaces of samples were polished and then partially covered with a protective mask in a series of strips. The samples were exposed to the ion flux from the discharge plasma, which eroded the unprotected areas. The mask was removed chemically and the erosion measured with a profilometer. Tests indicate that the sputter erosion rates of bulk metals obtained in a few hours agrees closely with those obtained in long-life tests.

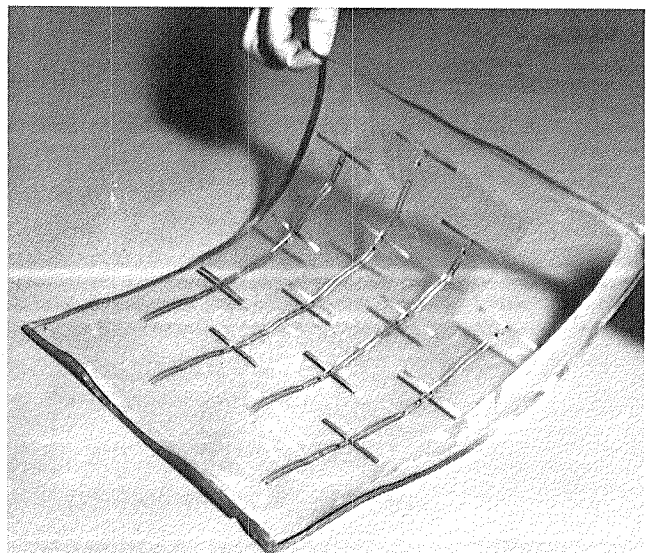
### **IR-100**

#### **Ultralightweight Printed-Circuit Rectenna**

A new ultralightweight, low-cost, flexible, 2.45-GHz, thin-film, etched-circuit "rectenna," making use of Kapton F film has been developed. This rectenna received an IR-100 award this year. This ultralightweight, high-efficiency converter of radio waves to dc power opens up many possibilities in power transmission without wires in aerospace and terrestrial applications, such as airplanes that do not carry fuel and can stay up for weeks at a time or spacecraft at high altitudes taking their power from a vehicle at a lower altitude. "Rectenna" is a functional abbreviation of the terms "rectifier" and "antenna" that denotes a special class of receiving antenna made up of continuous receiving cells each smaller in dimension than a wavelength and each terminated with a rectifying device. The output dc power then flows into the load. The resulting structure has a capture efficiency of nearly



*IAPS zenith module*



*Ultralightweight, printed-circuit rectenna*

100 percent. This rectenna offers higher conversion efficiency (85 percent) and lower specific weight (15:1 reduction) than conventional direct energy conversion devices. The specific power density of this element is 0.4 kg/kW for an incident energy density of 400 W/m<sup>2</sup>.

### Plasma Interaction Experiment (PIX-II)

Electrical interaction between space plasma and spacecraft systems are believed to cause various spacecraft anomalies. Lewis, other NASA Centers, and the Air Force have a coordinated program to explore the interaction phenomena. PIX-II, conceived, built, and qualified at Lewis, is a part of that program.

PIX-II will be launched late in 1982 as a piggyback experiment on the second stage of a Delta booster that will be placed in a 700-km polar orbit. The experiment will investigate and help to define the effect of space plasma on high-voltage solar arrays. The experiment package consists of a four-segment solar array and sun sensor on one side of the Delta stage and an enclosure box, Langmuir (potential) probe, and hot-filament probe mounted diametrically opposite. The probes are on deployable booms. The enclosure box contains an electrometer, a multiplexer-sequencer, Langmuir probe electronics, a high-voltage power supply, a power control unit, and a battery.

The experiment data, both stored and real time, will be telemetered to Lewis by the Delta downlink and the NASA tracking system. The Air Force will also receive and record the data and

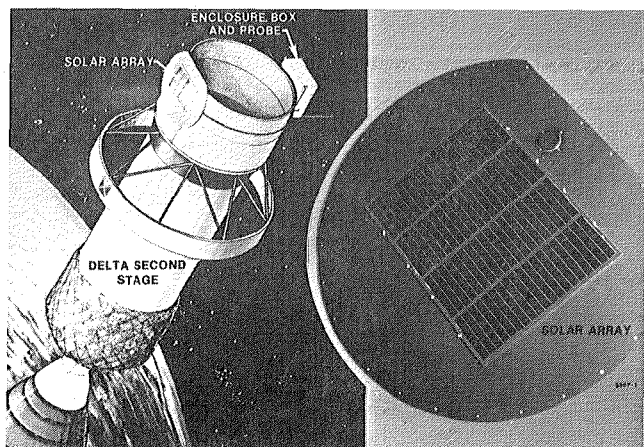
send Lewis the tapes. PIX-II should furnish investigators with the information needed to help understand undesirable and potentially harmful plasma interactions and should enable them to devise preventive measures.

### High-Frequency, High-Power Capacitor

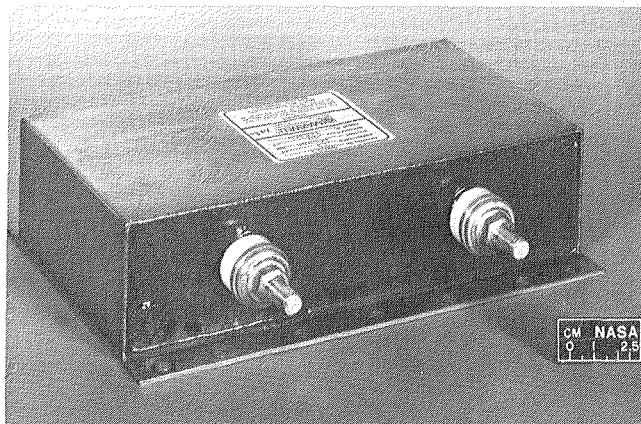
A 600-V, 125-A capacitor operating at 10 to 40 kHz has been developed by Maxwell Laboratories, Inc., under contract to Lewis. The capacitor has a reactive power rating of 75 kVAR and weighs 8 lb. The specific capacitor built, a 0.83 radio-frequency capacitor, was life tested in a vacuum at full load. This type of capacitor will be used in large space power systems (25 to 100 kW), where both the high current and high voltage capabilities are important. They also may be used in ground-based power applications such as high-power, high-frequency power supplies, induction heating machines, and filtering networks.

### Lightweight, High-Frequency Transformer

A lightweight (7 lb), 20-kHz, 25-kVA transformer with input voltage of 200 V and output voltage of 1500 V was developed by Thermal Technology Laboratory, Inc., under contract to Lewis. Characteristics of the transformer include high efficiency (99.2 percent), low specific weight (0.28 lb/kVA), continuous duty operation, low-leakage inductance, high reliability, and very good serviceability. The advanced technology that this transformer exemplifies is not limited to power transformers but can be readily applied to other types of power magnetic devices.



PIX-II

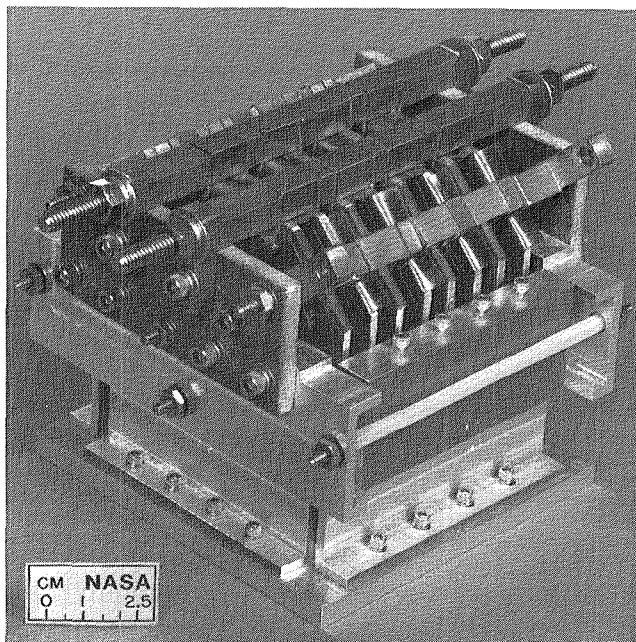


High-frequency, high-power capacitor

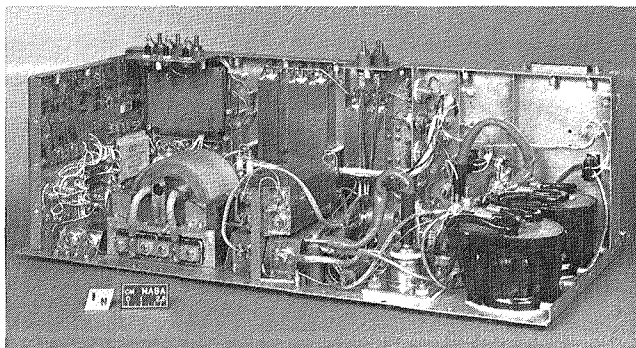


### High-Power Converter Modeling

High-power dc-to-dc converters are needed for advanced electric propulsion systems. Because of their potential advantages, series-resonant converters were investigated. As no comprehensive circuit models for this class of circuits existed in the literature, Lewis awarded grants to the University of Toledo to develop series-resonant circuit models. The University of Toledo derived and verified such models and is publishing them in journal articles. These models provide a better understanding of circuit operation, allow prediction of performance, and



*Lightweight, high-frequency transformer*



*High-power converter*

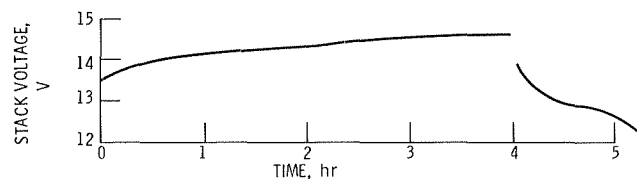
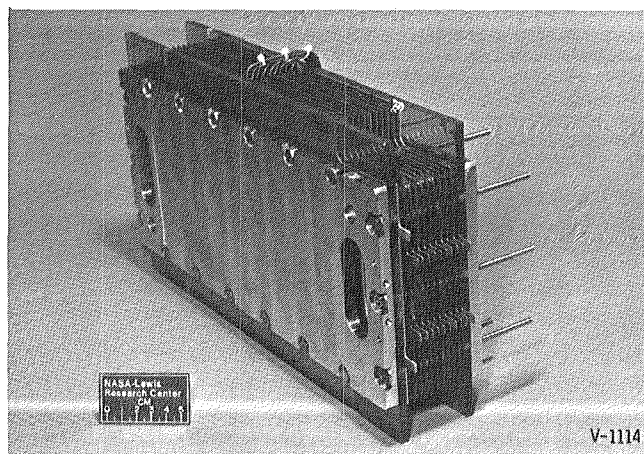
permit optimization of trade-offs. The way is clear to achieving lighter-weight higher-frequency converters. Although electric propulsion systems are the immediate beneficiaries of this new technology, it will also be applicable to large-space-structure power systems of the future.

### Advanced Power Conversion Technology

Electric power needs of future missions will require high-voltage, high-power converters. The development of these converters will be based on recent advances in power electronic components, such as high-power transistors. A recently developed high-power transistor was tested, characterized, and then incorporated in the design of a high-frequency, high-voltage, 10-kW power converter. Testing the developed converter verified that system benefits such as lower losses, less mass, and simplicity were achievable. This demonstrated power conversion technology is directly applicable to the power-conditioning needs of advanced electric propulsion systems and large space structures.

### Bipolar Nickel-Hydrogen Battery

Proof-of-concept testing has begun on a multicell stack of nickel-hydrogen cells. A



*Bipolar nickel-hydrogen battery and voltage variation*

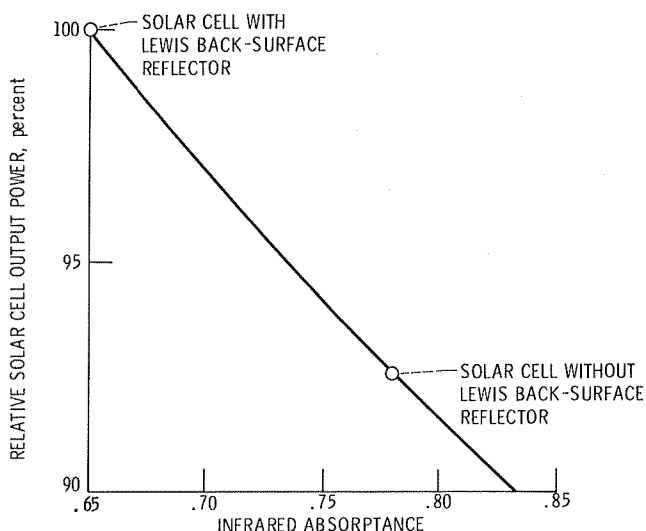


preliminary design suggested that nickel-hydrogen battery systems could be made by using constructional and assembly techniques that have been proven in the field of alkaline fuel cells. Significant improvements in gravimetric and volumetric energy density were indicated over batteries made by using current-state-of-the-art cells and technology. To verify these ideas, a 10-cell stack of nickel-hydrogen cells was assembled. The battery has been operated successfully. The 12-V, 6.5-A-hr device fits into a test chamber filled with hydrogen and is currently undergoing selective testing to determine battery performance. Battery characteristics being evaluated at Lewis are charge and discharge rate capability, cyclic joule and coulombic efficiency, cell-to-cell voltage and temperature variation, and self-discharge rates.

The results of the tests to date indicate excellent performance of the bipolar concept. Cyclic efficiency compares with that of conventional nickel-hydrogen cells. Because the cell-to-cell voltage variation is less than 0.003 V, each cell can be fabricated uniformly and thus battery performance is improved.

### Back-Surface Reflector for Silicon Solar Cells

It is known that solar cell power output decreases with increasing temperature. This results in less solar array power available to satellites in orbit. A significant cause of this



Increased power output from silicon solar cell with gold back-surface reflector

temperature increase is absorption of the Sun's infrared radiation by the metallic back contact of the solar cell. One scheme to alleviate this condition uses a back-surface reflector (BSR) under the cell's rear metallic contact. In research conducted at Lewis it was found that the most efficient back-surface reflector was a layer of gold under the cell's metallic rear contact. It resulted in a 16-degree drop in the silicon solar cell's operating temperature and an increase of about 8 percent in cell output power. A contractor has incorporated the Lewis-developed BSR into a thin, efficient solar cell that has passed thermal shock, contact adherence, and temperature-humidity tests. The increased power available from the silicon solar cell array can either increase satellite operating life or provide power for additional instrumentation on the satellite.

### Diamondlike Carbon Films

Ion beam, radiofrequency plasma, and vacuum arc deposition processes have been investigated at Lewis and found to produce carbon films that have many of the properties of diamond. The films can be made semitransparent, insulating, dense, hard, and chemically inert. Investigation into potential power technology application of these films is under way. Applications being considered include heat sinks for microwave devices, doped diamond semiconductors, and insulated gates for gallium arsenide semiconductors.



Ion beam sputter deposition system for making diamondlike carbon films

## Communications

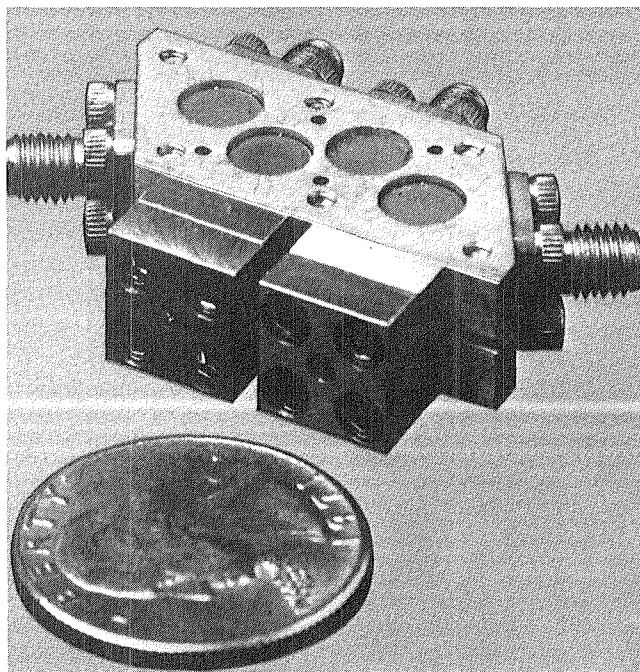
### Low-Noise Receiver for Advanced Communications Satellites

Considerable progress has been made toward the goal of developing reliable, efficient, low-noise receivers for use on NASA's Advanced Communications Technology Satellite. Two versions of such a receiver have been built under NASA sponsorship by LNR Communications, Inc., and by ITT and are now ready for testing. One key feature of these receivers is their low noise, which is anticipated to be around 6.5 dB. Receivers on previous Ka band communications satellites had noise as high as 11.5 dB. The receivers are also efficient, typically using 4 to 5 W of dc power.

These receivers are expected to be the proof of concept for flight-qualified receivers to be flown on the Advanced Communications Technology Satellite. They also will provide an advanced data base for use in communications payloads design and definition studies.

### Multibeam, Phased-Array Communications

Phased-array antenna systems on communications satellites have considerable

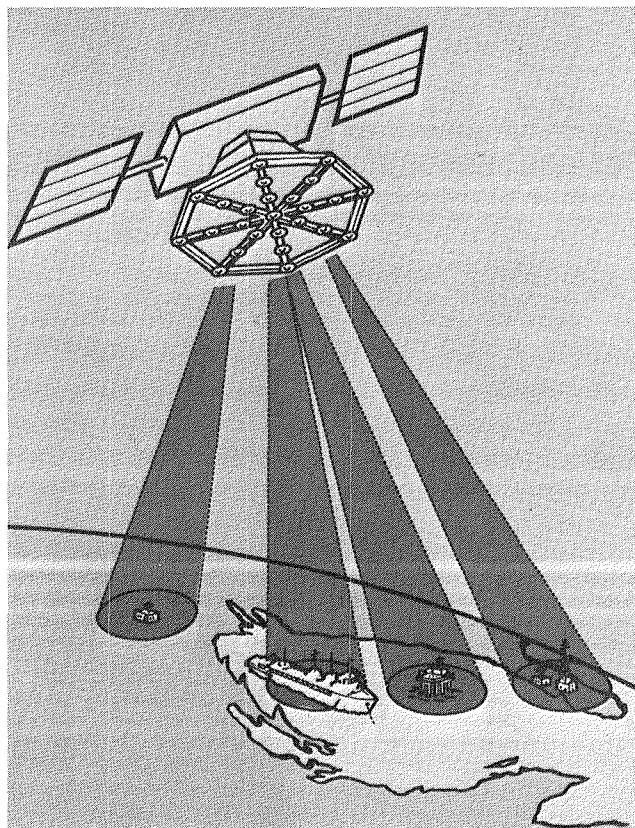


*Low-noise receiver*

potential for providing multiple beams, beam shaping, interference rejection, and operation with low-cost ground terminals. Eaton Corp. under contract to Lewis has completed the design, development, and ground demonstration of an adaptive, multibeam, phased-array communications experiment simulating a satellite operating in low Earth orbit. The system demonstrated forming and steering of transmitting and receiving beams, acquisition and tracking of simulated ground terminals, interference rejection, and multiple beam frequency reuse. This type of system can be used in maritime and aeronautical communications and data collection, with improved performance and increased spectrum utilization.

### On-Board Switching Unit for Advanced Communications Satellites

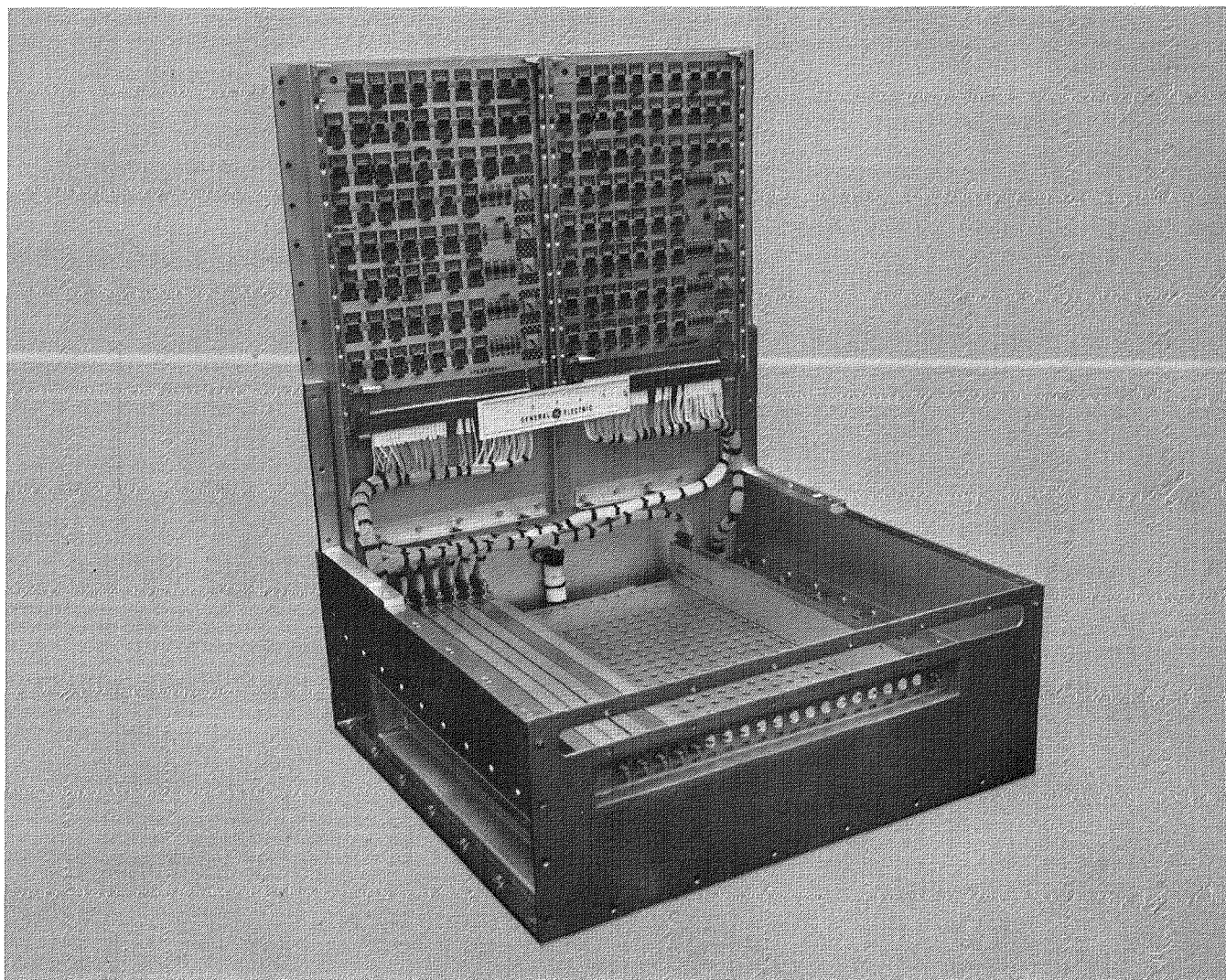
The next generation of communications satellites may use multibeam antenna systems and computer-controlled, on-board satellite



*Space application of adaptive multibeam phased array*

switching in order to interconnect many uplink beams (sending stations) to many downlink beams (receiving stations). The on-board satellite switching system will be similar to present ground-based switching systems in that it will consist of a complex array of switches (switch matrix) that are interconnected in such a manner that each uplink beam can be connected to each downlink beam. The satellite switch matrix, however, will differ significantly in appearance from its Earth-based counterpart because of packaging requirements for launch and space flight operation.

To explore the operational characteristics and identify the problems associated with space operation, the General Electric Co. and the Ford Aerospace Corp. have each designed and built, under contract to Lewis, switch matrices capable of interconnecting 20 uplink beams to 20 downlink beams (a  $20 \times 20$  switch matrix). These contracts are part of the NASA communications technology program to develop components suitable for operation in the 20- to 30-GHz frequency band. The GE and Ford units are similar in operational concept and switching architecture but different in overall package



*Switch matrix, showing output channels and control logic boards*



---

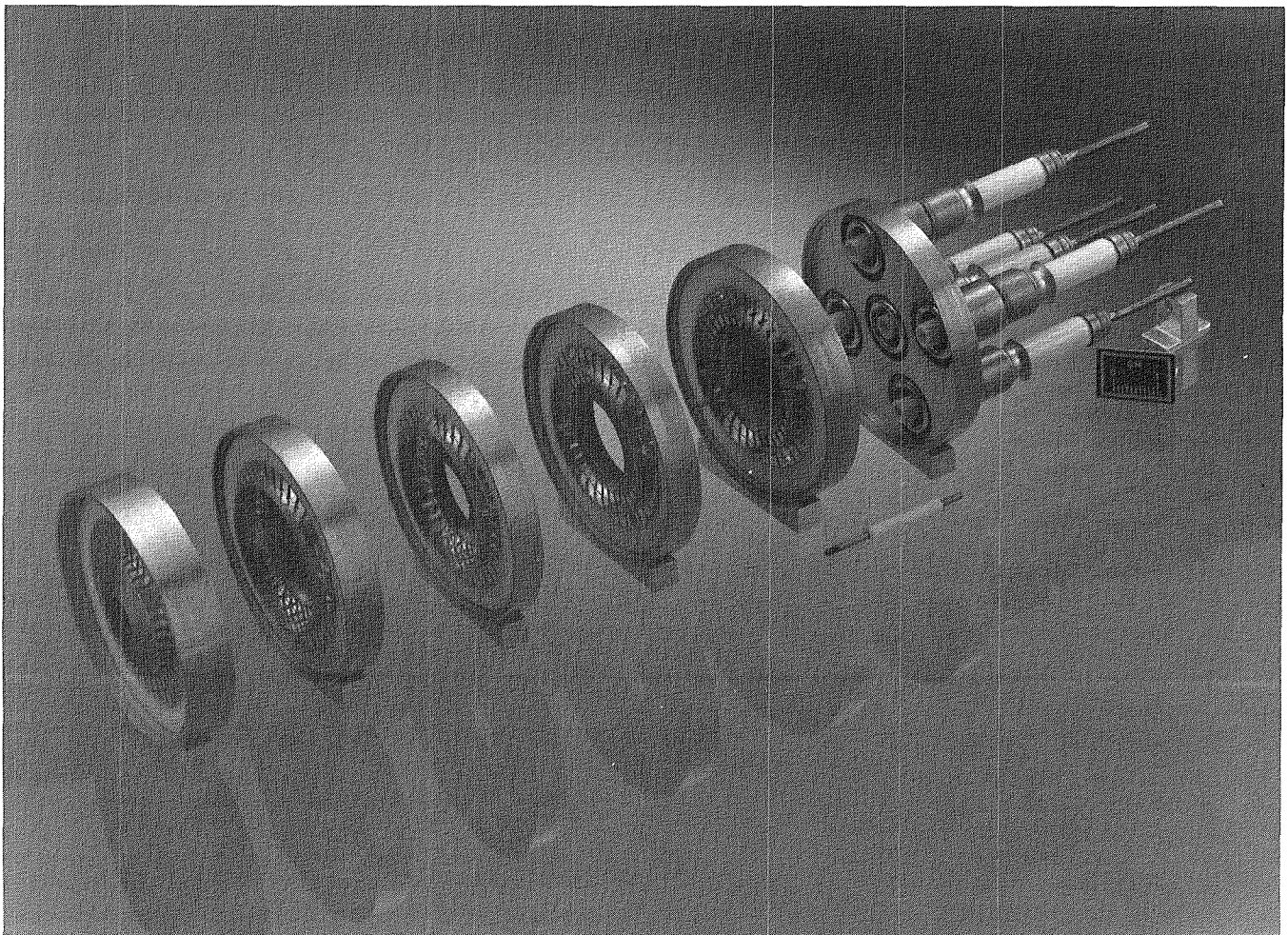
design and method of control.

Because of the high frequency of operation, the switch matrix can be designed by using high-technology miniaturized microwave design techniques and devices. For space application, the  $20 \times 20$  switch matrix, consisting of 800 couplers and 400 switching elements with transistorized driver circuit and control logic, can be packaged within a 20-in. by 20-in. by 5-in. enclosure that weighs less than 25 lb and requires less than 25 W of power.

#### **High-Efficiency Collectors for Traveling-Wave Tubes**

Significant progress has been made in developing ion-textured pyrolytic graphite for use

as multistage-depressed-collector (MDC) electrodes in traveling-wave tubes for space and aircraft applications. Because this strong, lightweight material has very low secondary electron emission characteristics, it produces higher collector efficiencies than are possible with conventional electrode materials such as copper. Ion-beam texturing studies with a number of materials, conducted at Lewis in 1976, first drew attention to the potential of secondary-electron-emission suppression effects with pyrolytic graphite. In addition, pyrolytic graphite has very high thermal emittance (also enhanced by texturing), high radial thermal conductivity, and high allowable operating temperatures, all of which permit good thermal control and high-power-density operation.



*Compact multistage-depressed-collector segments*

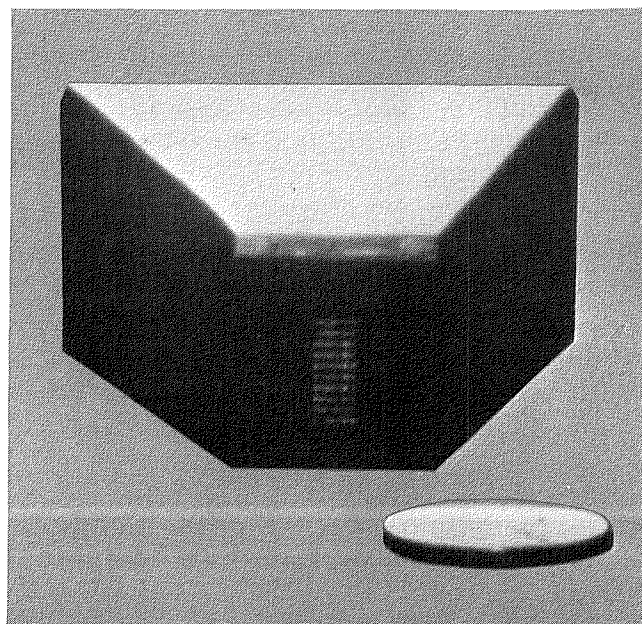
Under a contract to Lewis the Hughes Aircraft Co. has developed fabrication procedures to enable the use of pyrolytic graphite in brazed MDC assemblies. Compatible brazing materials and procedures were identified, along with material specification, inspection, and handling methods. A follow-on contract with Hughes is in progress to fabricate an MDC assembly, to retrofit it to an existing traveling-wave tube for space use, and to test and evaluate the resulting tube.

In-house efforts on this program at Lewis are progressing in three areas: (1) ion-texturing procedures have been significantly improved; (2) the secondary electron emission measurement procedures for the ion-textured pyrolytic graphite have been revised to more closely simulate actual collector surface operating conditions; and (3) a compact MDC assembly using pyrolytic graphite electrodes has been fabricated and successfully mated to and operated with an appropriate traveling-wave tube.

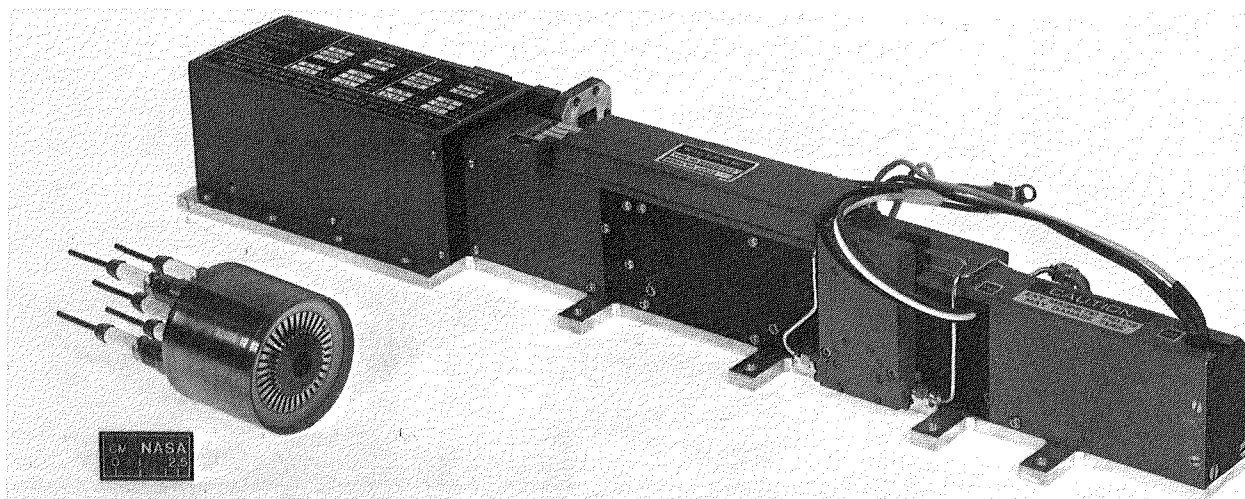
### Electro-Optical Processor

Carnegie-Mellon University, under a grant from Lewis, has been investigating the use of electro-optics technology to develop very high-speed computers. Optical signals travel at the speed of light and do not have some of the delays inherent in electronic computers. In one scheme devised at Carnegie-Mellon, an optical multiplier is connected to a conventional microprocessor. The optical multiplier can perform roughly 1 billion multiplication operations per second. The microprocessor is used to control light-emitting

diodes, which convert the electronic signals in the microprocessor to optical signals for the multiplier. The microprocessor is used to perform logical operations that cannot yet be done optically. During 1982, laboratory experiments showed that the electro-optical processor could solve some types of equations up to a thousand times faster than a conventional digital electronic computer.



*Optical multiplier*



*Multistage-depressed-collector assembly next to conventional collector portion of mating TWT*



Title	Lewis contact	Phone number, (216) 433-4000, extension	Headquarters program office
Low-Thrust Orbit Transfer	Raymond S. DiEposti	6655	OAST
Low-Thrust Chemical Rocket Engines	John P. Wanhainen	239	OAST
Simplified Prediction of Thrust Chamber Life	Harold J. Kasper	6893	OAST
Cooling with Hydrocarbon Fuels	Carl A. Aukerman	239	OAST
Eddy-Current Damping for Rotating Machinery	Robert E. Cunningham	6117	OAST
Improved Ion Thruster Performance	* James S. Sovey	5183	OAST
Ion Auxiliary Propulsion System	James F. DePauw	6119	OAST
Rapid Measurement of Sputter Erosion	Vincent K. Rawlin	6664	OAST
Ultralightweight Printed-Circuit "Rectenna"	James E. Triner	5221	Director's Discretionary Fund OAST
Plasma Interaction Experiment (PIX-II)	Louis R. Ignaczak	6652	OAST
High-Frequency, High-Power Capacitor	David D. Renz	6663	OAST
Lightweight, High-Frequency Transformer	Gene E. Schwarze	5233	OAST
High-Power Converter Modeling	Robert P. Gruber	260	OAST
Advanced Power Conversion Technology	Robert J. Frye	6851	OAST
Bipolar Nickel-Hydrogen Battery	Robert L. Cataldo	364	OAST
Back-Surface Reflector for Silicon Solar Cells	Henry B. Curtis	309	OAST
Diamondlike Carbon Films	Bruce A. Banks	491	OAST
Low-Noise Receiver for Advanced Communications Satellites	Gerald J. Chomos	746	OSSA
Multibeam, Phased-Array Communications	Richard J. Krawczyk	6851	OSSA
On-Board Switching Unit for Advanced Communications Satellites	Ernie W. Spisz	746	OSSA
High-Efficiency Collectors for Traveling-Wave Tubes	Arthur N. Curren	6865	OAST
Electro-Optical Processor	Robert J. Baumbick	6136	OAST

# Terrestrial Energy

---

## **Ceramic Stators Successfully Tested in Rapid Thermal Cycling**

High-strength structural ceramics, such as silicon carbide and silicon nitride, have great potential for use in advanced gas turbine engines. These ceramics have greater high-temperature strength and better oxidation resistance than superalloys, but the ability of ceramic engine components to withstand the rapid thermal cycles required for automotive gas turbine application was unknown. A study was conducted by Ford Motor Co., under DOE-NASA sponsorship, to evaluate the behavior of ceramic stators produced by four ceramic suppliers. The stators were tested in a computer-controlled hot flow rig that simulated both the cyclic temperatures and airflow rates typical of an automotive driving cycle. The test rig was cycled at a rate of 1 cycle/min from an idle condition at 1300° F to a maximum temperature of 2200° F for one series of tests and to a maximum of 2500° F for another series of tests.

Both silicon nitride and silicon carbide survived the hot flow rig tests. In the 2200° F tests one silicon nitride component survived almost 500 hr of testing and 30,000 cycles. In the 2500° F tests a silicon nitride stator and a silicon carbide stator each survived 150 hr of testing and 9000 cycles with no failures. The results demonstrated that ceramic turbine components could successfully withstand the severe thermal transients that

would be encountered in automotive gas turbine engines.

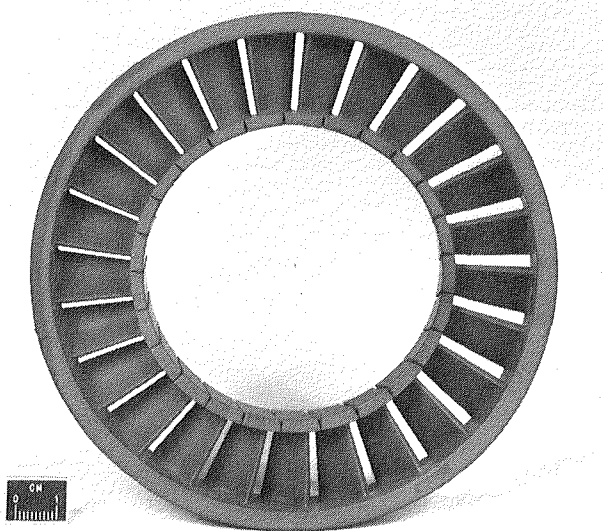
## **Low-Emission Combustor for Automotive Turbine Engine**

As part of the Department of Energy's Automotive Technology Development Program, Lewis is working to develop a technology base applicable to an automotive gas turbine engine. Lewis has contracted with the Detroit Diesel Allison Division of General Motors Corp. and with the Garrett Turbine Engine Co. for this purpose. Objectives of this program include a 30 percent mileage improvement over comparable 1985 spark-ignition engines and emissions levels below Federal research objectives. Development of a ceramic premixed, prevaporized combustor is critical to meeting these objectives.

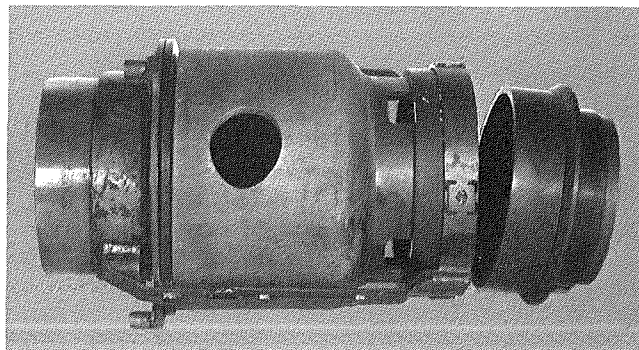
During 1982 a ceramic combustor, suitable for engine use, was rig tested at air inlet temperatures to 1835° F and resulting gas temperatures to 2250° F. Emissions levels were well below the program objectives. The ceramic combustor hot section includes five alpha silicon carbide pieces and has variable geometry to accommodate the automotive driving cycle from idle to full power. The ceramic combustor has operated for more than 16 hr over a wide range of conditions, including startup and acceleration transients, with no damage sustained. Because of the rig success a ceramic combustor is included in the first engine build.

## **Advanced Turbocompounded Diesel Engine**

To reduce highway vehicle fuel consumption, the Department of Energy (DOE) is investigating ways to recover exhaust waste heat from heavy-duty diesel truck engines. As manager of a



*Ceramic stator typical of those tested in hot flow rigs*



*Low-emission ceramic combustor*

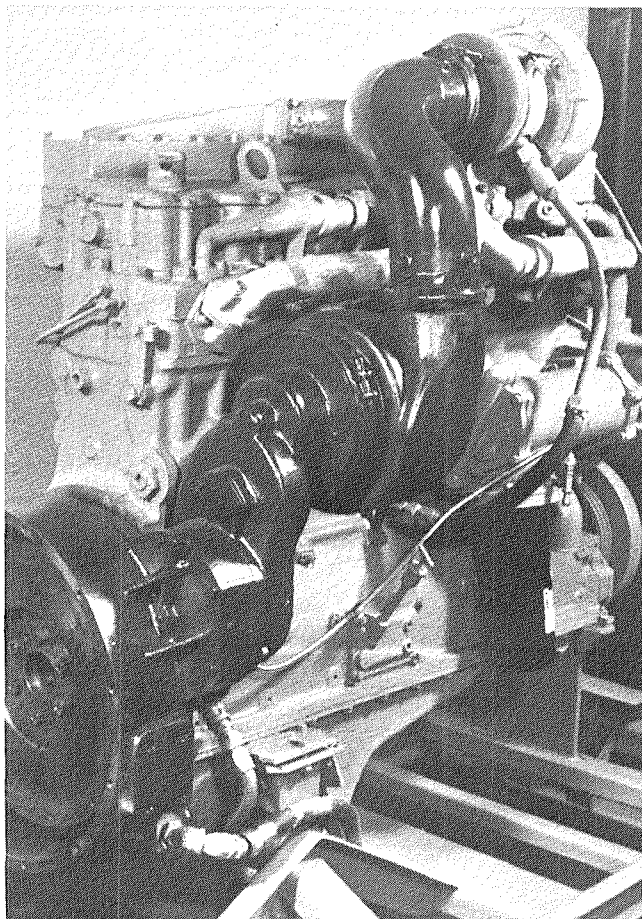
project in support of DOE, Lewis contracted with the Cummins Engine Co. to investigate turbocompounding as one means of exhaust gas heat recovery. Turbocompounding uses an exhaust turbine to recover useful energy from the exhaust gas of a reciprocating engine. It differs from the use of a free-floating turbocharger in that "compounding" mechanically couples the recovered power to the engine drive train.

An advanced form of the original turbocompounded engine developed by Cummins recently demonstrated an additional 6.5 percent improvement in fuel economy over the original engine. The goal for this program was 5 percent. The improvement was obtained primarily by redesigning and insulating the exhaust system between the turbine and the engine, by using ball bearings on the high-speed turbine shaft, by matching the turbine and engine speeds better,

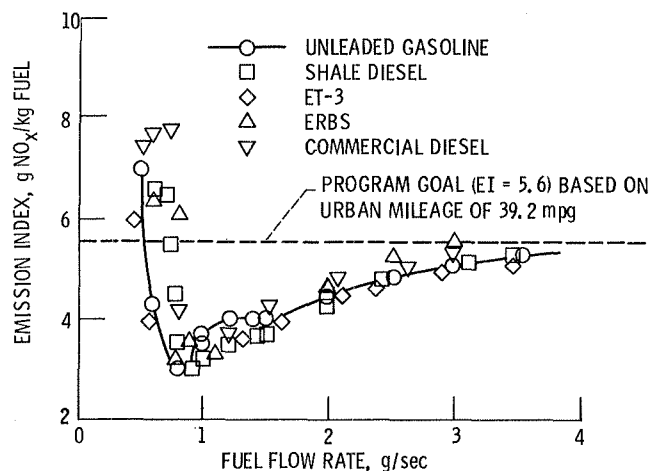
and by using a new engine camshaft profile. The advanced engine, like the original, still managed to meet the California emissions standard for heavy-duty vehicles.

### Automotive Stirling Engine Development

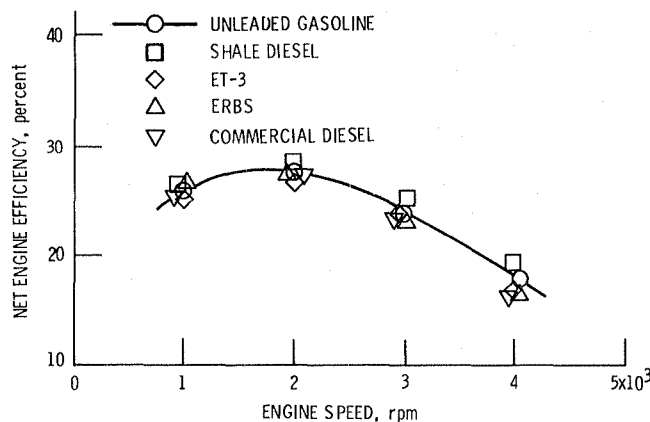
One benefit of the automotive Stirling engine would be to provide an automobile that operates reliably on a wide variety of fuels. A "workhorse" Stirling engine recently demonstrated its fuel versatility. Without any hardware changes, this engine operated successfully on unleaded gasoline, commercial automotive diesel fuel, marine diesel derived from shale oil, a broadened-specification aircraft gas turbine fuel, and commercial gasohol. Engine power, efficiency,



Turbocompounded diesel engine



Stirling P-40 NO<sub>x</sub> emissions during multifuel testing

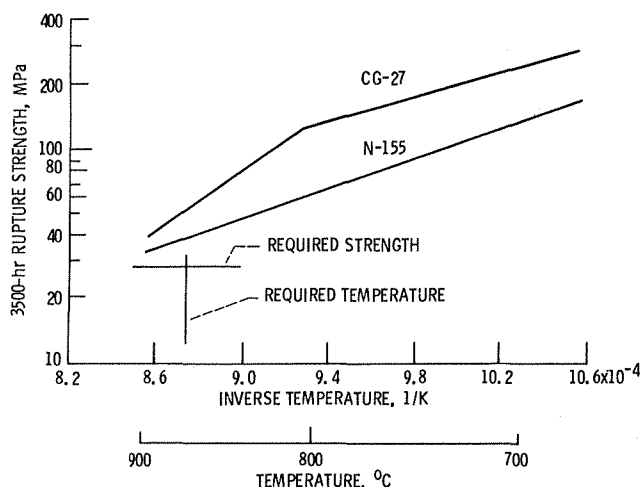


Stirling P-40 net engine efficiency during multifuel testing

and exhaust emissions were essentially identical for all fuels.

### Iron-Base Alloy for Stirling Engine Heater-Head Tubes

Automotive Stirling engines require heater-head tubes that must contain the hydrogen gas working fluid at high temperatures (1600° F) and also resist high internal pressures as well as an



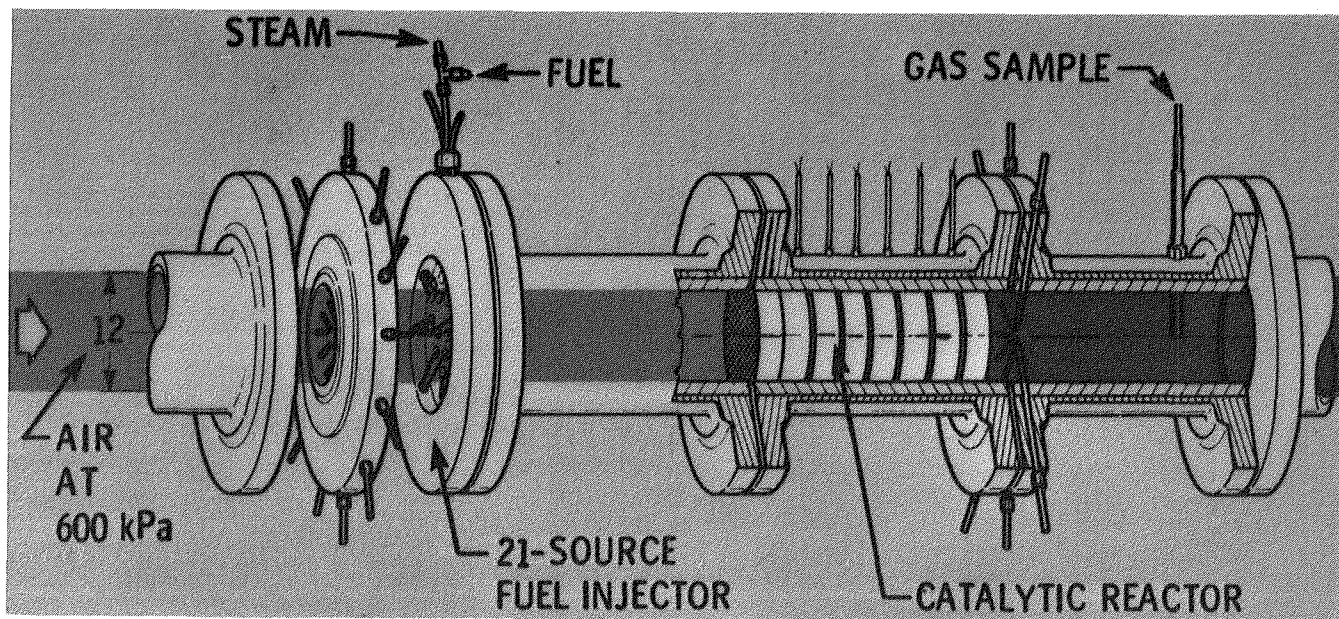
3500-hr rupture strength comparison for CG-27 and N-155

external oxidizing-corrosive environment. The alloy currently in use contains the strategic metal cobalt and thus is expensive. A materials research and technology effort in support of the DOE-NASA Lewis Automotive Stirling Engine Project was undertaken to replace the currently used alloy with a lower cost alloy that would still meet the severe operating requirements of the automotive Stirling engine.

Candidate heater-head tube alloys were evaluated for oxidation and corrosion resistance, high-temperature creep-rupture strength, endurance under simulated engine operating conditions, and resistance to hydrogen loss by permeation through the thin tube walls. The commercial alloy CG-27 was shown to be superior to the alloy now in use (N-155) in all of these categories. In addition, CG-27 is less expensive and does not contain the strategic metal cobalt. A heater-head quadrant has been fabricated with CG-27 heater-head tubes and is now being tested on a Stirling engine under conditions anticipated for advanced automotive engines.

### Catalytic Combustion with Steam Injection

Stationary-power gas turbine engines for utility and industrial applications currently require high-quality, scarce, and therefore costly fuels such as



Steam-injected catalytic combustor

natural gas and petroleum distillates. These engines are also subject to stringent Federal and local control of oxides of nitrogen ( $\text{NO}_x$ ). Research is currently under way to develop the technology for burning more readily available fuels, such as residual oils, in an environmentally acceptable manner.

Catalytic combustion has demonstrated that low  $\text{NO}_x$  levels well within environmental standards can be achieved with many fuels. However, use of residual oils results in unacceptable upstream burning.

An experimental combustor study was conducted at Lewis to determine if residual oil catalytic combustion could be improved by injecting steam, along with the fuel, upstream of the catalytic reactor. Steam is often readily available for such usage in stationary-power installations.

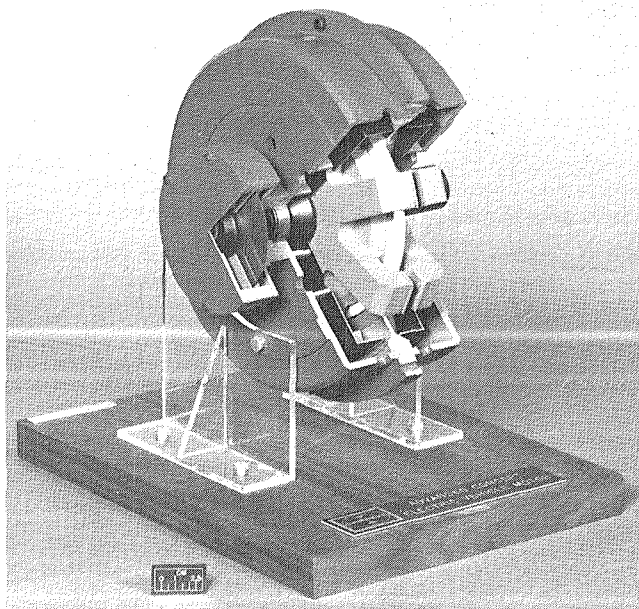
The injection of steam prevented upstream burning from taking place if the steam flow rate was at least 30 percent of the airflow rate. Inspection of the test duct after the tests showed all of the surfaces to be free from fuel deposits. Tests without steam injection had resulted in the coating of fuel injector surfaces, premixing duct walls, and even catalytic reactor surfaces with fuel deposits when inlet temperatures were below 800 K.

The major effect of steam injection is believed to be better fuel atomization, which causes fuel droplets to follow air streamlines and thereby retards fuel deposition on premixing duct walls. As a result, upstream burning is avoided.

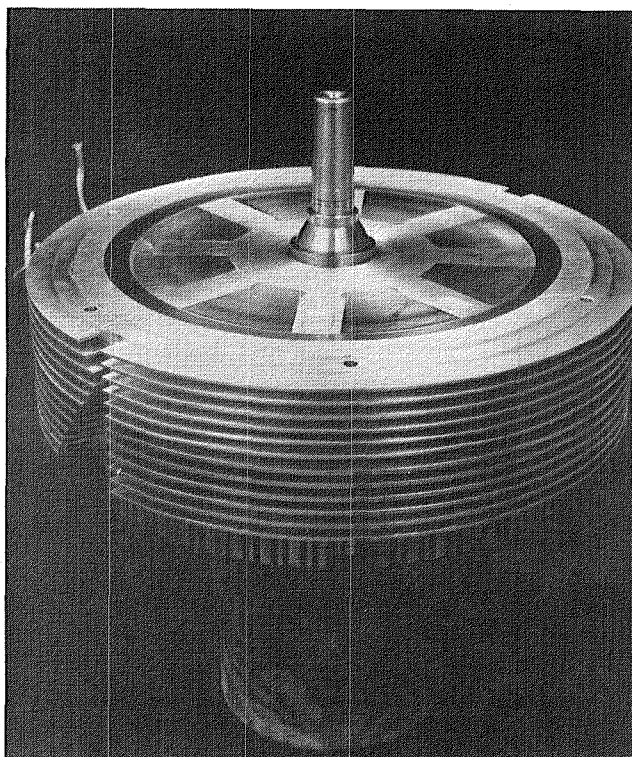
### Advanced Motors for Electric Vehicles

The present state of the art of propulsion motors for electric vehicles relies on brush commutation and electromagnetic excitation. These motors are too heavy, typically around 100 kg, and too expensive, from \$1000 to \$4000, for an economical vehicle. They also require brush commutator maintenance. As part of the Department of Energy's Electric and Hybrid Vehicle Program, Lewis has developed electronically commutated, permanent-magnet-excited advanced propulsion motors under contract.

Two air-cooled motors of a disk (axial gap) configuration with high-energy permanent magnet excitation have been tested in full-rated laboratory test models. One motor, developed by the General Electric Co., uses multiple magnets and has demonstrated 93 percent efficiency at a power density of 0.35 kW/kg. The other,



Advanced motors for electric vehicles





---

developed by AiResearch Corp., uses a single large magnet and has demonstrated 88 percent efficiency at a power density of 0.63 kW/kg. These motors, because of their simple construction, have potential for low cost. Their disk configuration extracts penalties in increased inertia and losses, but these penalties may be acceptable in many applications.

### **Nondestructive Testing of Transistors**

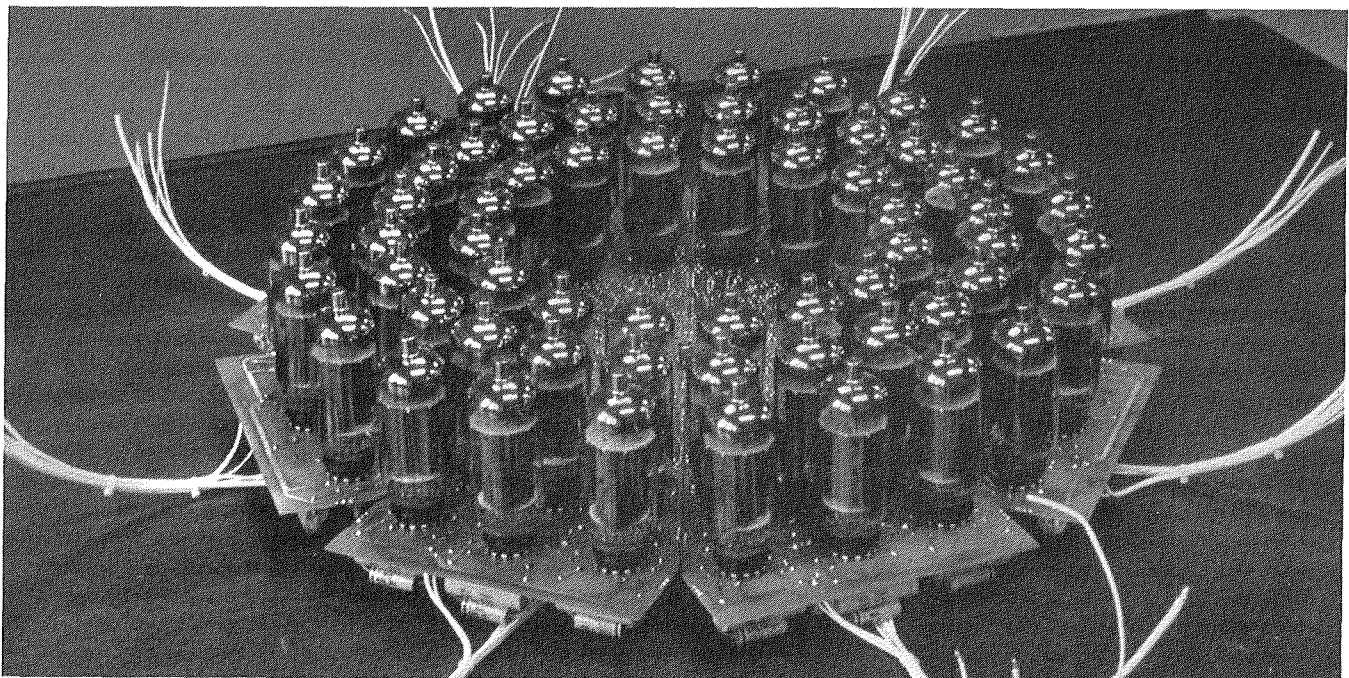
Suitable characterization of new high-power transistors is essential to the design of lightweight, efficient, reliable motor controllers, dc-to-ac inverters, and other power electronic circuits. Of particular concern is the transistors' safe operation during the switching of high currents. Conventionally, determination of the safe switching capability of a transistor requires a test that usually results in transistor failure—a costly process since high-power transistors can cost \$400 or more. As part of the Electric and Hybrid Vehicle Propulsion Development Project managed by Lewis for the Department of Energy's Electric and Hybrid Vehicle Program, Virginia Polytechnic Institute, under a grant, has developed an apparatus for nondestructive characterization of a transistor's safe switching

capability to 120 A. This apparatus, using an array of high-speed vacuum tubes, diverts current away from the transistor at the inception of breakdown during switching and thereby prevents damage and provides needed data at low cost.

### **Large-Wind-Turbine Cluster**

In support of the Federal Wind Energy Program, directed by the Department of Energy (DOE), Lewis managed the development of the Mod-2 wind turbine. A cluster of three Mod-2 machines is in operation at Goodnoe Hills, Washington. Each Mod-2 has a 300-ft-diameter rotor and produces 2500 kW of energy at a wind speed of 20 mph. The three-machine cluster is currently providing power to the Bonneville Power Administration utility network. The Mod-2 machines were designed, assembled, and installed at Goodnoe Hills by the Boeing Engineering and Construction Co. under contract to Lewis.

The three Mod-2 machines are being used to define wind characteristics within wind turbine wakes, to determine wake effects on cluster performance, and to measure structural dynamic loads. The machines were installed in a triangular planform that provides a separation between



*Apparatus for testing high-power transistors*

---

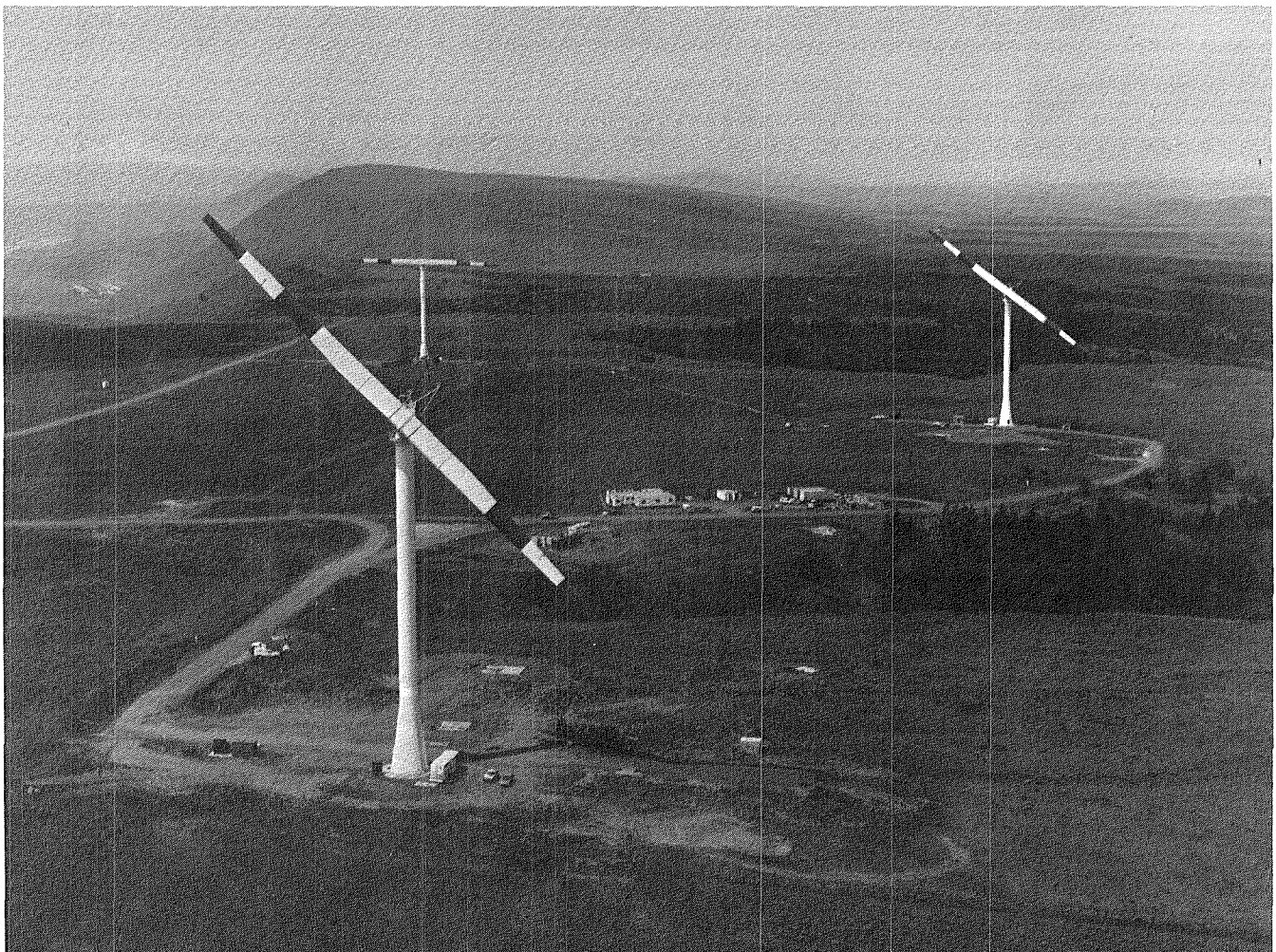
machines of 1500, 2100, and 3000 ft. The machines, in this planform, provide a unique facility for conducting these tests. Other current research includes aeroacoustic measurements and dynamic control effects on wind turbine system behavior. The results of this research will be generalized and reported to enable designers to better evaluate the siting of larger numbers of wind turbines in a cluster. Installations of large clusters of wind turbines are currently being planned by state and commercial consortiums.

#### **Advanced Electrocatalysts for Phosphoric Acid Fuel Cell Powerplants**

Under a Lewis advanced research contract to synthesize better electrocatalysts, Stonehart

Associates has developed a platinum alloy that promises improved performance at lower cost. The new catalyst for anode usage is a platinum-palladium alloy highly dispersed on a high-surface-area corrosion-resistant carbon support. The alloy has been prepared and tested in the laboratory and is the subject of a patent application filed by the Department of Energy.

Present-technology fuel cells require about 1 g of anode platinum for each kilowatt of electric power produced. This quantity of platinum, worth \$14 when platinum is \$450 per troy ounce, can be replaced with \$5 worth of the platinum-palladium alloy. This is a savings of \$9 per kilowatt produced. There is no loss of efficiency or long-term stability.



*Large-wind-turbine cluster*

### 40-kW Phosphoric Acid Fuel Cell Powerplant Field Test

The first 40-kW phosphoric acid fuel cell, on-site powerplant of a joint Department of Energy-Gas Research Institute (DOE-GRI) field test project was installed in April 1982 at a commercial laundry in Portland, Oregon. Lewis is the program lead center for the DOE Phosphoric Acid Fuel Cell Program. This powerplant is the result of a multiyear DOE-GRI engineering and development project. Forty-five more 40-kW-fuel-cell powerplants will be delivered to test sites throughout the United States from a Lewis-managed contract with United Technologies Corp. The contract will also provide field engineering support and limited spare parts for each powerplant during 1 yr of field test operation by the various participating utilities.

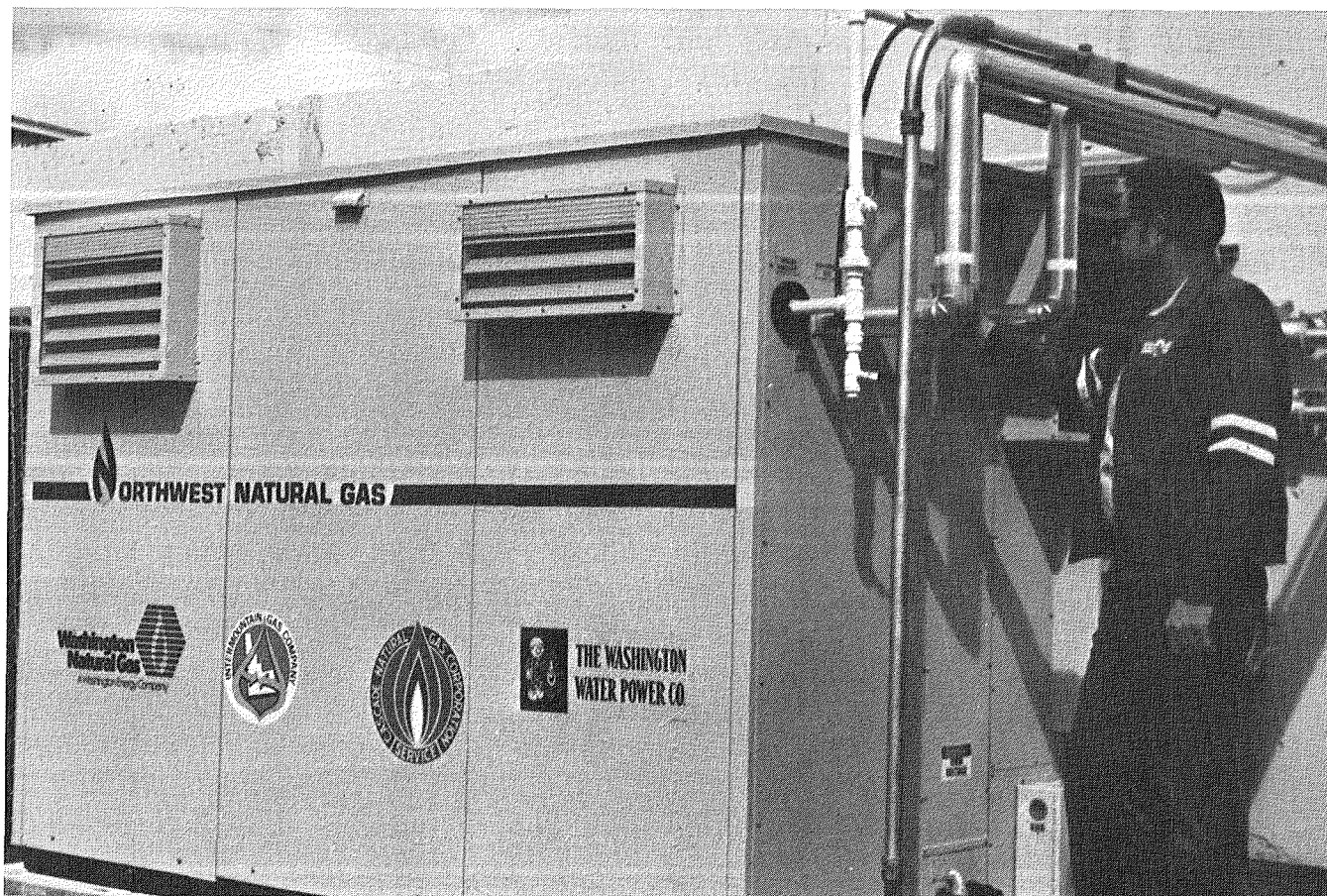
The 40-kW, on-site powerplant can provide

electricity and heat at the point of use to apartments, commercial buildings, and light industrial plants. The overall efficiency of the powerplant operating at one half to full capacity is approximately 80 percent. The laundry will use all the heat from the powerplant, and electricity not needed at the site will be sold to the local power company.

Northwest Natural Gas Company of Portland, Oregon, is the operating utility for a consortium of utilities that includes Washington Natural Gas Co., Intermountain Gas Co., Cascade Natural Gas Co., and the Washington Water Power Co.

### Ceramic Coatings for Utility Gas Turbines

The Electric Power Research Institute (EPRI) and Lewis have recently completed a joint program to assess the potential of thermal barrier coatings for improving the durability and



40-kW fuel cell powerplant installed at site

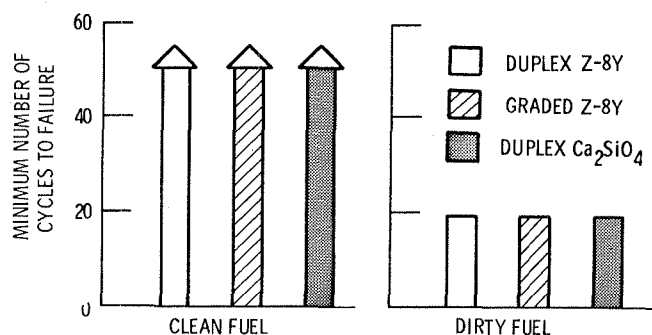


efficiency of gas turbines. Coatings were evaluated in clean fuel and in simulated low-quality, dirty fuel over a range of temperatures typical of utility gas turbine service. The key test involved cycling of coated specimens in a 9-atmosphere pressurized passage. In this test a good simulation of transient and steady-state thermal stresses was accomplished. A startup and shutdown cycle faithful to utility practice and a much more severe stepped startup-shutdown cycle were run. For both types of cycles, duplex and graded zirconia-8-wt% yttria coatings and a calcium silicate duplex coating survived in clean gas turbine no. 2 fuel but failed in less than 20 cycles in dirty fuel. From this result and the results of a 4000-hr ambient-pressure clean fuel test, where graded coatings fared poorly, it was concluded that duplex ceramic thermal barrier coatings are ready for the further development required to carry out utility field tests.

In an allied program, under the Advanced Conversion Technology (ACT) Project funded by the Department of Energy, several duplex ceramic thermal barrier coatings were tested by Solar Turbines, Inc., in their Mars gas turbine for 500 hr

in clean fuel. Calcium titanate, zirconia-8-wt% yttria, and calcium silicate coatings performed quite well considering the first-stage blade geometry and the minimal effort expended in developing coating application techniques for each coating system.

Further development of coating application technology is required before the potential of ceramic coatings in stationary gas turbines will be realized.



*Ceramic coating lives at high pressure in clean and dirty fuels*

Title	Lewis contact	Phone number, (216) 433-4000, extension	Headquarters program office
Ceramic Stators Successfully Tested in Rapid Thermal Cycling	Gordon K. Watson	434	OAST
Low-Emission Combustor for Automotive Turbine Engine	Paul T. Kerwin	770	OAST
Advanced Turbocompounded Diesel Engine	James C. Wood	6632	OAST
Automotive Stirling Engine Development	Frank J. Kutina	343	OAST
Iron-Base Alloy for Stirling Engine Heater-Head Tubes	Joseph R. Stephens	6676	DOE reimbursable
Catalytic Combustion with Steam Injection	David N. Anderson	715	Energy Systems Division
Advanced Motors for Electric Vehicles	Balazs R. Hatvani	5214	OAST
Nondestructive Testing of Transistors	Edward A. Maslowski	5214	OAST
Ceramic Coatings for Utility Gas Turbines	Stanley R. Levine	6150	OAST
Large-Wind-Turbine Cluster	Bradford S. Linscott	6106	Energy Systems Division
Advanced Electrocatalysts for Phosphoric Acid Fuel Cell Powerplants	Milton R. Lauver	767	OAST
40-kW Phosphoric Acid Fuel Cell Powerplant Field Test	Rudolph A. Duscha	5241	OAST

**End of Document**